Spatial Structure Modulates Persister Formation in A Synthetic Cross-Feeding Bacterial Community

A DISSERTATION
SUBMITTED TO THE FACULTY OF THE GRADUATE SCHOOL
OF THE UNIVERSITY OF MINNESOTA - TWIN CITIES

BY

Xianyi Xiong

IN PARTIAL FULFILLMENT OF THE REQUIREMENTS
FOR THE DEGREE OF
MASTER OF SCIENCE

Advisors: William R. Harcombe Ph.D.
Hans G. Othmer, PhD. (Co-Advisor)

May 2022

ACKNOWLEDGEMENTS

I would like to express my special appreciation to Advisor Professor Will Harcombe and Co-Advisor Professor Hans Othmer, who have been continuous sources of inspiration to my graduate career in bacterial systems biology research. Both of them inspire me to use scientific research as an avenue to create societal impact, but they also constantly remind me that research is a step-by-step effort. I would like to thank other members on my Faculty Thesis Committee (see below). I thank Professor Satoshi Ishii for being my scientific mentor since we first met in 2019. I also thank Professor Ryan Hunter and Professor Jeff Gralnick for their support throughout my master's career.

I would also like to thank Professor Dan Knights (Dept. of Computer Science and Engineering) and Professor Abigail Johnson (School of Public Health) for providing me an opportunity to do a research rotation with them and connect my microbial ecology research to clinical areas. Folks in the Harcombe Lab (Dr. Jon Martinson, Dr. Jeremy Chacón, Ave Bisesi, Dr. Sarah Hammarlund, etc) also gave me invaluable guidance and feedback throughout my research.

Finally, I would like to thank Haining Zhou, Ziyi Jia, Wen Cai, Zhiyue Wang, Jinyi Chen, Andrew Baldys, and Grace Zhang, Xun Yuan—great friends and family who have been by my side over the last several years. I could not have done it without you.

FACULTY THESIS COMMITTEE

Thesis Advisor: William Harcombe, Ph.D.
Academic Title: Associate Professor of Ecology, Evolution, and Behavior; John & Abigail Wardle Chair in Microbial Ecology, BioTechnology Institute

Thesis Co-Advisor: Hans Othmer, Ph.D.
Academic Title: Professor of Mathematics, School of Mathematics

Thesis Committee Member: Satoshi Ishii, Ph.D.
Academic Title: Associate Professor of Soil, Water, and Climate, BioTechnology Institute

Thesis Committee Member: Ryan Hunter, Ph.D. (On Sabbatical)
Academic Title: Associate Professor of Microbiology and Immunology, Medical School

Alternative Thesis Committee Member: Jeff Gralnick, Ph.D.
Academic Title: Professor of Plant and Microbial Biology

ABSTRACT

Antibiotic persistence is an important mechanism that allows bacteria to survive antibiotic stress. Persistence also contributes to the evolution of antimicrobial resistance (AMR), which played a role in ~5-million death worldwide in 2019 alone. The role that microbial ecology plays in antibiotic persistence remains largely unknown. Here, I studied the effect that cross-feeding on agar surfaces has on antibiotic persistence. Using an obligate cross-feeding mutualism of engineered strains of *Escherichia coli* and *Salmonella enterica*, I discovered that in the spatially-structured environment, the antibiotic persister frequency in *E. coli* was ~100-fold higher in the cross-feeding coculture than in monoculture. This heightened *E. coli* persister frequency was removed (1) when *E. coli*'s metabolic dependency on *S. enterica* was broken through metabolite supplementation, and (2) when the growth environment was spatially homogeneous in the shaken liquid medium. Using high-throughput quantification of the *E. coli* growth physiology on agar, I found that average growth rate was not sufficient to explain the heightened *E. coli* antibiotic persistence in mutualism. By pairing the single-colony analysis with a PDE mathematical model on growth physiology, I found that the high persistence phenotype in the cross-feeding coculture is correlated with increased variability in both growth rate and lag time, and future effort will be needed to determine their relative contributions. Together, my thesis showed that the combination of cross-feeding and spatial structure is a novel mechanism which increased phenotypic heterogeneity in bacterial growth and persistence to antibiotics. Finally, my work implies the potential clinical threat of antibiotic persistence in spatially-structured polymicrobial infection sites. The experimental setup in this work is also foundational to incorporate spatial structure into the study of the highly debated relationship between mutualism and community stability.

TABLE OF CONTENTS

LIST OF TABLES

LIST OF FIGURES

CHAPTER I: INTRODUCTION & LITERATURE REVIEW

I.1. Post-Antibiotic Era: Antibiotic Resistance, Tolerance, & Persistence

I.1.1. The Post-Antibiotic Era is Marked by Antibiotic Treatment Failure

Humanity is entering a "post-antibiotic era" (Reardon, 2014; WHO, 2014), where minor infections can once again kill even with antibiotic treatment. Antibiotic treatments will increasingly fail, requiring higher antibiotic dosage or different antibiotics to control infections (Garcia, 2009; Tillotson et al., 2020). In fact, this trend has been true for the past few decades. The overall antibiotic failure rate increased on average by 12% in the UK between 1991 and 2012 (Currie et al., 2014). Together with this trend, about 4.95 million deaths world-wide in 2019 alone were associated with bacterial resistance to antibiotics, which is responsible for more death than HIV/AIDS or malaria (Antimicrobial Resistance Collaborators, 2022). Antibiotics that used to be effective are losing their efficacy, and we need better understanding of the processes contributing to this pattern and how to combat them.

Antibiotics are losing their efficacy because bacteria evolve strategies that overcome antibiotic stress (Bush et al., 2011). The most well-known strategy is antibiotic resistance (Windels et al., 2020). Two other less-researched, yet vital, strategies are antibiotic tolerance and antibiotic persistence (Lewis, 2010; Balaban et al., 2019). Despite recent research on antibiotic tolerance and persistence, almost all studies neglect the fact that bacteria typically live in complex microbial communities where they interact ecologically with many other species (Ratzke et al., 2020). Even less research has investigated the spatial dynamics of interspecies interactions and the interplay with antibiotic tolerance/

persistence. In my thesis, I aimed to close an important knowledge gap around how cross-feeding interactions regulate antibiotic persistence in a spatially-structured microbial mutualism. Closing this gap may result in a microbial ecology-informed clinical strategy for treating bacterial infections, so that we may slow down the ever-increasing rate in antibiotic treatment failure and postpone the post-antibiotic era.

I.1.2. Antibiotic Resistance Can Underlie Antibiotic Treatment Failure

Antibiotic resistance is a major cause of antibiotic treatment failure (Cunha & Ortega, 1995). Antibiotic resistance describes the ability of bacteria to **grow** in continuous antibiotic stress (Windels et al., 2020), so prescribing patients with antibiotics that the pathogenic bacteria are resistant to is bound to cause treatment failure. Thus, clinics and public health agencies are continuously screening bacterial isolates from bacteria-infected patients for antibiotic resistance to ensure correct antibiotic prescription.

A common measurement of antibiotic resistance is the minimal inhibitory concentration (MIC), which is the lowest concentration of antibiotics needed to inhibit growth (Andrews, 2001). Growth of bacteria in liquid growth media can lead to accumulation of biomass and cell number, and will lead to turbidity in the bacterial culture (Buss da Silva et al., 2019). Fig.1.1a shows a common protocol for assessing MICs. Both wild-type and resistant bacterial cells are seeded at a low density into a series of wells with growth media and gradually-increasing concentrations of antibiotics. After appropriate incubation, turbidity will be checked for each well. The lowest concentration at which turbidity is absent will be considered the MIC. Clearly, resistant (Res) bacteria

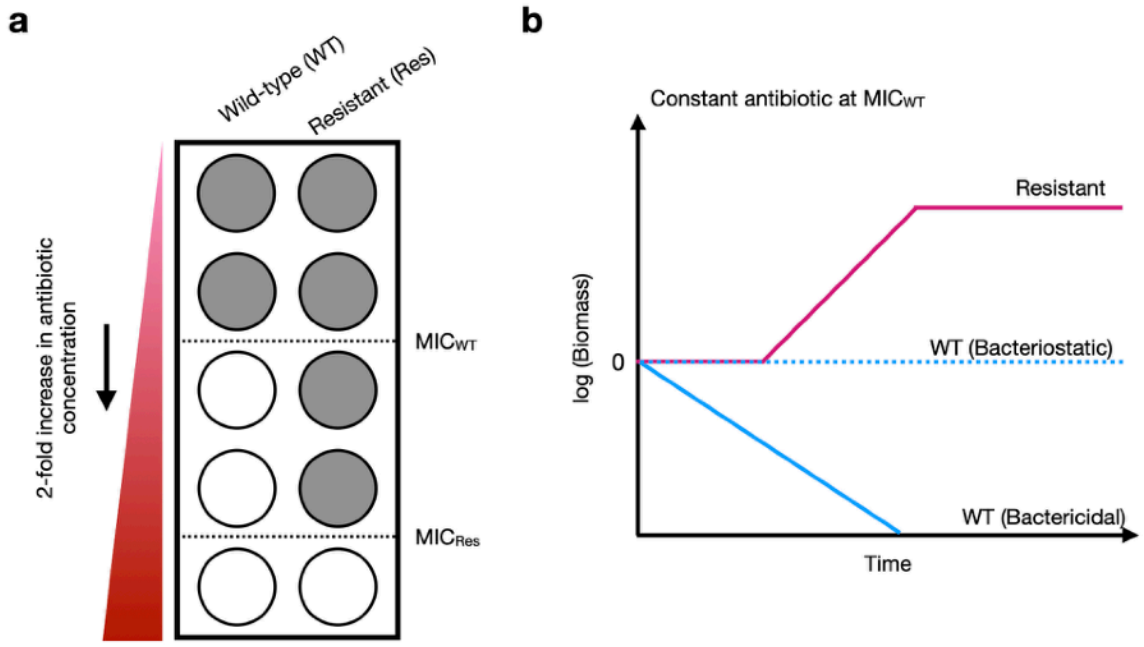

Figure 1.1. Antibiotic Resistant Bacteria Grow in Higher Concentrations of Antibiotics. a Minimum inhibitory concentration (MIC) is commonly used to measure antibiotic resistance. Resistant bacteria (Res) can grow in higher concentration of antibiotics than wild-type cells (WT), so we have $MIC_{Res} > MIC_{WT}$. Turbidity (shown in grey) indicates bacterial growth. **b** For wild-type bacteria, bactericidal antibiotics reduce their survived cell biomass, whereas bacteriostatic antibiotics prevent growth but cause no death. Resistant bacteria will grow and result in an increase in biomass in antibiotic concentrations of MIC_{WT}.

have a higher MIC than wild-type (WT) ones, that is, $MIC_{Res} > MIC_{WT}$.

The non-turbid wells are wells that lack bacterial growth, which can be due to either death or maintenance of the current cell number. When wild-type bacterial cells are challenged with **bactericidal** antibiotics, the cell number will exponentially decrease (Fig. 1.1b). But with **bacteriostatic** antibiotics, the cell number will maintain relatively unchanged with no significant increase. The population dynamics of wild-type bacteria with antibiotic challenges can be contrasted with the counterpart in the resistant bacteria, which will follow a logistic growth after a short non-growing lag time. This ability of resistant bacteria to grow in non-lethal concentrations of antibiotics was first observed by Alexander Fleming soon after he discovered antibiotics (Fleming, 1945), and the

biological mechanisms of antibiotic resistance have been thoroughly studied since then.

As summarized in Table S1 (Appendix I: Supplementary Literature Review), the genetic and biochemical mechanisms are well-known due to research effort to understand antibiotic resistance (aka "antimicrobial resistance," "AMR"; Munita & Arias, 2016). AMR is usually reflected by features in the bacterial DNA (Reygaert, 2018). The genetic mechanisms of AMR focus on how bacteria gain resistance through changes in DNA sequence, whereas biochemical mechanisms are about how the resistance-causing genetic information eventually leads to the resistant phenotype (e.g. observable increase in MIC of a bacterial strain).

Even though AMR plays an important role in causing antibiotic failure, it is not the only mechanism we should care about. Antibiotic tolerance and antibiotic persistence are two other mechanisms that have recently been shown to be clinically relevant causes for antibiotic treatment failure (Liu et al., 2020), yet their mechanisms remain relatively less studied.

I.1.3. Antibiotic Tolerance/Persistence Also Can Cause Antibiotic Treatment Failure

Antibiotic tolerance and persistence can also cause antibiotic treatment failure. Unlike antibiotic resistance, tolerance and persistence are meaningful terms only to describe how bacteria respond to killing by bactericidal antibiotics. **Antibiotic tolerance** is defined as a process of dying more slowly in the presence of antibiotics (Fridman et al., 2014). In contrast, **antibiotic persistence** refers to the presence of a subpopulation of transiently antibiotic-tolerant cells within a bacterial population (Balaban et al., 2019). By

definition, neither tolerant nor persistent bacteria can grow in bactericidal antibiotics. So their MICs are similar to the susceptible populations (Fig. 1.2a). To distinguish between tolerance and persistence, microbiologists rely on distinct features of the kill curves of bacteria under continuous treatment of the bactericidal agents.

Tolerance and persistence are measured as the minimum duration for killing (MDK) a significant portion of the bacterial population by a specific antibiotic. Tolerance can be reliably assessed by the metric MDK_{99} (Brauner et al., 2017), where the time it takes to kill 99% of a population is tracked (Fridman et al., 2014). As shown in Fig. 1.2b, microbiologists can track the survival rate of the population over time to draw the bacteria's "kill curve", and use this curve to deduce MDK_{99}. Note that both the

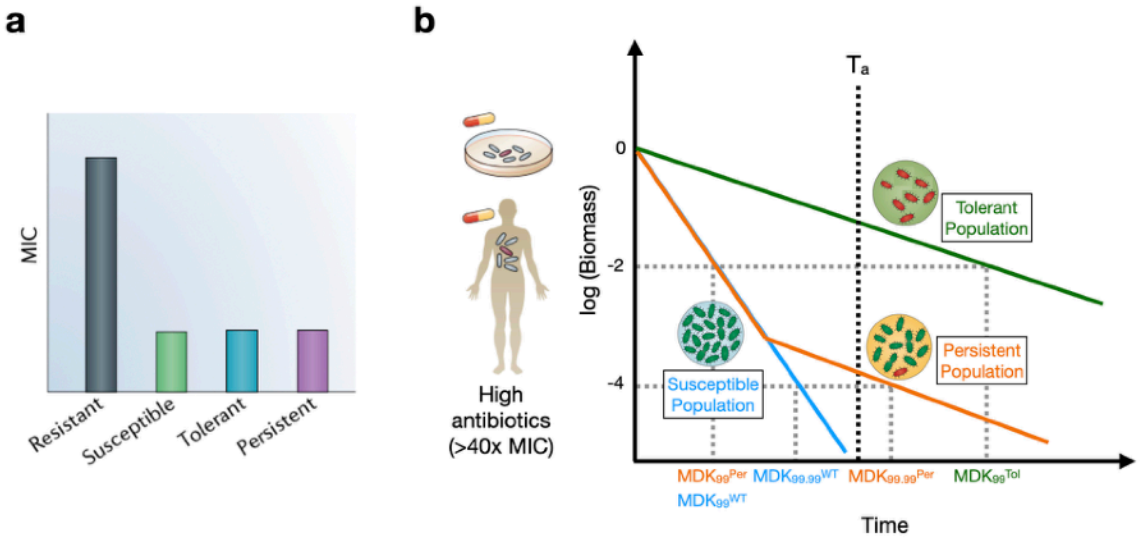

Figure 1.2. Distinguishing Antibiotic Tolerance and Antibiotic Persistence. a Both the tolerant and persistent populations have the same antibiotic resistance as the susceptible population and can be distinguished from the resistant population (measured by MIC). Figure 2a in Balaban et al. (2019) was reproduced here. **b** Tolerance and persistence are measured as the minimum duration of killing 99% and 99.99% of the bacterial population, respectively (MDK_{99} and $MDK_{99.99}$). The persistent population has the same tolerance as the susceptible one, but has a different persistence than the susceptible population. The tolerant population has a higher tolerance than the susceptible one. Note that the kill curve for the susceptible population ends right before the hypothetical antibiotic treatment time, T_a, when the population dies off. The indication of using high-concentration antibiotics to perform the killing experiment (>40x MIC) was reproduced from Figure 1b in Balaban et al. (2019).

susceptible and tolerant populations follow a simple exponential death rate, but their death rates are different so they differ in tolerance ($MDK_{99}^{Tol} > MDK_{99}^{WT}$). In contrast, persistence can be assessed by measuring $MDK_{99.99}$, the time it takes to kill 99.99% of the population (Balaban et al., 2019). A persistent population includes a subpopulation of antibiotic tolerant cells with a different death rate than the rest of the population. Thus, the kill curve of a population with persisters is biphasic (Fig. 1.2b), with the less steep phase denoting the killing of the tolerant subpopulation. As a result, both the persistent and susceptible populations have the same tolerance ($MDK_{99}^{Per} = MDK_{99}^{WT}$). The two populations only differ in persistence ($MDK_{99.99}^{Per} > MDK_{99.99}^{WT}$).

To test for antibiotic tolerance and persistence, microbiologists have to use antibiotic at a high concentration—typically at least several times the MIC of the tested bacteria—for continuous treatment. For example, the conventional test for tolerance and persistence requires the use of ampicillin as the bactericidal antibiotic at a concentration of 100 μg/mL, which is >40 times the MIC of the model microorganism *Escherichia coli* (Fig. 1.2b). There are two reasons for using a high antibiotic concentration. First, using a high enough antibiotic concentration can prevent heteroresistance in a bacterial population from confusing death rate calculations. **Heteroresistance** arises when subpopulations of cells have a higher MIC than the majority of the population (Balaban et al., 2019). If dosed at a concentration that is just above the MIC, the heteroresistant subpopulation may still grow, and this will confuse the calculation of bacterial survival fractions in determining tolerance and persistence. Second, the bacterial death rate is dependent on

the concentration of the bactericidal antibiotic (e.g. penicillin) and this rate plateaus at a high-enough concentration (Eagle & Musselman, 1948). Using a high enough antibiotic concentration also rules out the possibility that the biphasic killing appears due to antibiotic degradation in the absence of persister cells.

Both antibiotic tolerant and persistent bacterial populations can lead to antibiotic treatment failure. Demonstrated conceptually in Fig. 1.2b, the entire susceptible population has died off by a hypothetical duration of antibiotic treatment, T_a, whereas some fractions of the tolerant and the persistent populations survive T_a. After the antibiotics get cleared out due to reactions with the bacterial cells or to metabolism in the human body, the surviving bacteria can grow again and maintain infection. In a milestone paper, Liu et al. (2020) found that methicillin-resistant *Staphylococcus aureus* (MRSA) isolates from two life-threatening blood infection cases in the clinic showed increases in tolerance but not in resistance, demonstrating the relevance of antibiotic tolerant cells in causing treatment failure in clinics.

Despite their clinical relevance, antibiotic tolerant bacteria have received little attention until the last decade. One explanation may be that antibiotic tolerant bacteria are not nearly as important as antibiotic resistant ones, so receive less clinical attention. But as Levin-Reisman et al. (2017) have shown, antibiotic tolerant cells can eventually evolve to become resistant.

I.1.4. Tolerance and Persistence Can Ultimately Lead to Antibiotic Resistance

Antibiotic tolerant cells—whether as a subpopulation or as an entire population—

can evolve to gain AMR-related mutations in antibiotic treatment. Levin-Reisman et al. (2017) first made this ground-breaking discovery *in vitro* in their evolution experiment that cyclically exposed *E. coli* bacteria to growth medium with high- and low-concentration antibiotics. This novel experimental evolution protocol was developed to simulate the living condition of infectious bacteria during clinical antibiotic treatment, where the high-dosage oral antibiotic administration every 5~8 hours leads to high concentration in the human body, which is followed by a low concentration due to the human body metabolism.

Levin-Reisman et al. (2017) characterized the *E. coli* isolates from the end of this evolution experiment and discovered resistant *E. coli* strains. These *E. coli* isolates gained resistance by at least 5-times MIC through mutations in the promotor of the *ampC* gene encoding beta-lactamase, which was known to increase *ampC* expression (Jaurin & Normark, 1983). In early cycles of the experiment, the authors found non-resistant *E. coli* strains with mutations that increased lag time—known as "tolerance-by-lag" or "tbl" mutations and are a major mechanism for tolerance (Fridman et al., 2014). These tbl mutants can stay longer in a non-growing, and therefore, non-dying lag phase against the cell wall inhibitor ampicillin (Lee et al., 2018). By performing whole-genome sequencing on *E. coli* populations along different cycles of the evolution experiment, Levin-Reisman et al. confirmed that the AMR mutations always appeared on genetic backgrounds of the tbl mutations.

Finally, Levin-Reisman et al. (2017) developed a probability-based mathematical

model to understand why the AMR mutations always appear on tolerant backgrounds. By parameterizing the model, the authors discovered that resistance mutations are >10-fold more likely to establish on the tolerant background than on the wild-type one. This occurs because tolerant mutations have a wide target size whereas the successful, one-step AMR mutations were almost restricted to the *ampC* promoter region in the *E. coli* strain used for experiments, supporting earlier evidence (Girgis et al., 2012). In another word, the tolerant genetic background ensures survival of bacterial strains such that the rare, yet key, resistance mutations can occur.

Subsequently, the antibiotic-tolerant clinical MRSA cells that Liu et al. (2020) isolated from patients were also evolved in this cyclical exposure protocol *in vitro* to high- and low-concentrations of antibiotics, and were found to evolve AMR much faster than their non-tolerant counterparts. Taken together, results in Liu et al. (2020) and Levin-Reisman et al. (2017) emphasized that antibiotic tolerant mutations can quickly evolve due to a larger mutational target size for tolerance than for resistance, and that AMR mutations are likely to establish when appearing on the tolerant background. Given the clinical importance of antibiotic tolerant bacterial cells, it is necessary to perform more research to understand them.

Despite their significance in contributing to AMR, antibiotic tolerance and persistence still receive much less attention by the scientific community compared to AMR. One potential reason is that most tolerant mutants—whether dominating the population or remaining a subpopulation—end up becoming resistant and get classified

clinically as resistant mutants. Beyond illuminating the link between antibiotic tolerance and resistance, results from the evolution studies above were also seminal to our understanding that antibiotic tolerance can form due to genotypic changes and is genetically stable—just like AMR. In contrast, what mechanisms contribute to antibiotic persistence remain largely under-explored, warranting future research.

I.2. Phenotypic Heterogeneity: Mechanisms for Antibiotic Persistence

Antibiotic persistence has been known to microbiologists since early 1940s. Hobby et al. (1942) and Bigger (1944) were the first to observe and characterize the non-resistant, low-frequency *Staphylococcus pyogenes* bacteria survivors of >24h penicillin treatment at a near-clinical concentration. Bigger then called these survivors "persisters" for their phenotype to persist antibiotic stress without dying. Since then, the process of persister formation—i.e. how the persister phenotype arises—has been researched upon. It was originally thought that they were non-dividing, dormant cells that were tolerant to bactericidal antibiotics (Bigger, 1944). Interestingly, it was later found that not all dormant cells were antibiotic-tolerant (Orman et al., 2013), but persister frequency was enriched in the physiologically dormant fraction of the population (Lewis, 2005). In reality, many more complex qualitative changes in these dormant cells underlie persister formation (Harms et al., 2016). Importantly, researchers were able to attribute antibiotic persistence to a key mechanism called "phenotypic heterogeneity."

Phenotypic heterogeneity is foundational to our understanding of antibiotic persistence. Phenotypic heterogeneity is the "phenotypic diversity that occurs

independently of genetic or environmental variation and thus manifests between genetically identical individuals that live in the same microenvironment" (Ackermann, 2015). Naturally, the isogenic bacterial populations can be phenotypically heterogeneous even when grown in the same microenvironment. For example, individual *E. coli* cells have been found to grow at different rates within the same growth medium (Kiviet et al., 2014). A major task in understanding antibiotic persistence has been to understand how phenotypic heterogeneity can be attributed to genetic mutations (Section I.2.1), stochastic gene expressions (Section I.2.2) and physical mechanisms (Section I.2.3).

I.2.1. Genetic Mutations Can Underly Persistence

I start by reviewing the genetic mechanisms contributing to the persistence phenotype as a subpopulation-level tolerance. In the early years of antibiotic persistence research, microbiologists wanted to find a genetically stable strain of *E. coli* with a high persister fraction so that they could characterize these sub-population level persister cells. The first strain they found was the *hipA7* mutant strain of *E. coli* (Moyed & Bertrand, 1983), which has a ~1000-fold higher persister frequency than the wild-type (Balaban et al., 2004). This mutant allowed microbiologists to link antibiotic persistence with the toxin-antitoxin (TA) module in many bacteria (Korch et al., 2003).

The TA module plays an important role in governing the bacterial dormancy state, which in turns leads to antibiotic persistence. The TA module encodes for a toxin protein (e.g. HipA) causing dormancy in bacterial cells—a bacterial physiology state where metabolism is reduced without causing cell death—and an antitoxin (e.g. HipB) that

counteracts the toxin activity (Song & Wood, 2020). The HipA toxins can trigger growth arrest in bacteria by inducing the biosynthesis of (p)ppGpp (guanosine pentaphosphate), a secondary messenger responsible for stringent stress response in many bacteria (Bokinsky et al., 2013). The produced (p)ppGpp then reshapes bacterial physiology by reprogramming transcription and halting growth and metabolism so that cells enter dormancy. Meanwhile, (p)ppGpp can further change the target protein activities, such as up-regulating *hipA* expression (Hauryliuk et al., 2015). Increased ppGpp level leads to accumulation of inorganic polyphosphate (Kuroda et al., 1997), which then allows the protease Lon to degrade antitoxins such as HipB and free active toxin molecules (e.g. HipA; Kuroda et al., 2001), forming a closed cycle to reinforce persister formation.

The detailed molecular pathways of persister formation paved ways for understanding the role of genetic mutations in causing phenotypic heterogeneity. As hypothesized in Rotem et al. (2010), the *hipA7* mutation may lead to less effective binding between HipA and HipB to neutralize the HipA toxicity and thus higher persister frequency (Vazquez-Laslop, et al., 2006). This hypothesis was supported as the authors observed that a substantial fraction of *hipA7* colonies appeared on LB agar much later (i.e. longer lag time) than the rest of the population, and that there was no shift of the appearance time for the rest of the population. Together, these data indicated higher heterogeneity in terms of the cellular state regarding dormancy, rather than simply a shift in the average value. Further, the authors provided data from the Fluorescence Resonance Energy Transfer (FRET) microscopy experiment to validate that the HipA7-HipB binding

was significantly less efficient than that of HipA^{WT}-HipB. All these results suggested that the weakened HipA7-HipB binding was sufficient to cause an effective fraction of the *E. coli* cells to have less toxin inhibition, which led to higher persistence but not tolerance.

Other genetic mutations were also found to be associated with a heightened antibiotic persistence—not tolerance—in bacteria. Examples include the knockout mutation of the *metG* and *hipB* genes in *E. coli* (Girgis et al., 2012). However, whether these mutations led to an increased heterogeneity in the *E. coli* populations has not been mechanistically elucidated. Regardless, one question remained unanswered why persisters existed in *E. coli* with wild-type HipA-HipB binding in the first place.

I.2.2. Stochastic Gene Expression Underlies Antibiotic Persistence

One explanation for the existence of persister cells in wild-type *E. coli* with regular HipA-HipB binding was stochastic gene expression. Stochastic gene expression is "manifested as fluctuations in the abundance of expressed molecules [e.g. proteins] at the single-cell level, and variability and heterogeneity within populations of genetically identical cells" (Kærn et al., 2005). This heterogeneity in the number of free HipA proteins has been shown to contribute to persister formation (Rotem et al., 2010). The authors controlled the *hipA* gene expression with tetracycline induction on a plasmid in *E. coli*. The authors found that there was a larger fraction of cells with an extended lag time (dormancy) as the induction level of *hipA* expression became higher.

Rotem et al. (2010) further found that the cells became dormant if their HipA toxin level was higher than a threshold, and the variability in HipA levels among cells led to a

coexistence between persister and growing cells. The persister fraction could be captured by a stochastic (i.e. Monte Carlo) simulation of the fraction of cells with free HipA level higher than the threshold. These result suggested that the degree of persistence can be controlled phenotypically under the same genetic background of bacteria. As Harms et al. (2016) concluded, stochasticity in *hipA* expression in a bacterial population (even when the average expression level was low) can lead to cells with high free HipA toxin concentrations and is sufficient to explain why only a *fraction* of cells are persisters.

Most recently, single-cell, temporal analysis of bacterial growth and stress response gene expression established a substantial link between stochastic gene expression and predisposition to survive antibiotic stress (Sampaio et al., 2022), which may underlie antibiotic persistence as a differential survival mechanism. The authors tracked gene expression of *E. coli* using fluorescent markers before a short lethal ciprofloxacin treatment, and compared the pre-antibiotic expression profile and growth rate between survived and killed cells. Interestingly, a pulse of elevated expression of the *gadX* gene responsible for acid resistance appeared together with a period of slow growth in survived cells (Sampaio et al., 2022), supporting the previous idea that "transcriptional bursting" contributes to stochastic gene expression and persistence (Kærn et al., 2005).

Moreover, stochastic gene expression is believed to also be affected by environmental conditions. Given the nature of persister formation as a stringent response, microbiologists have categorized persisters into two groups: (1) triggered and (2) spontaneous persisters (Balaban et al., 2019). Triggered persisters form due to a pre-

exposed stress (e.g. antibiotic treatment, starvation, pH change), whereas spontaneous persisters are produced stochastically when the bacteria are in steady-state exponential growth. It was thought that even though little stress and abundant nutrient are present in the exponential phase of bacterial growth, "microstarvation" can occur to a very small fraction of the bacteria and causes them to become persisters (Harms et al., 2016). By this logic, more starvation or stress is thought to take place in stationary-phase cultures and is consistent with the fact that triggered persisters are much more frequently encountered than the spontaneous ones (Balaban et al., 2004; Balaban et al., 2019). Common triggers leading to starvation or stress include chemicals such as salicylate (Wang et al., 2017) and long-term starvation in a bacterial culture (Levin-Reisman et al., 2010; Orman et al., 2013). Such starvation in bacterial culture was also shown to cause a fraction of cells to gain increased dormancy (Levin-Reisman et al., 2010).

Finally, a lot of research has shown that antibiotic persistence is affected by the function of many genes, proteins, and pathways, and by the challenge of numerous chemical stress (Harms et al., 2016). Therefore, the Pash (aka PaSH, "persistence as stuff happens) hypothesis was posited to state that persisters are "an inadvertent product of different kinds of errors and glitches," and can hardly be linked to specific genes (as reviewed in Levin et al., 2014). This hypothesis was supported by a recent study (Kaplan et al., 2021) that examined the mechanism guiding persister formation when bacteria were challenged with acute stress.

I.2.3. Persister Formation in Bacteria Due to Acute Stress

Recent results in Kaplan et al. (2021) supported the Pash hypothesis. The authors discovered that antibiotic persistence can be explained by bacterial cells stochastically becoming metabolically frustrated and entering growth arrest. Kaplan et al. (2021) provided evidence that acute stress can lead to a halt in metabolism in random members of the *E. coli* bacterial population, who then became persisters and survived the lethal antibiotic treatment. Furthermore, the antibiotic survival fraction of the *E. coli* population can be predicted by the duration of the acute stress.

Experimentally, Kaplan et al. (2021) treated exponential-phase *E. coli* with an acute serine hydroxamate (SHX) stress to cause serine starvation and growth arrest (Potrykus & Cashel, 2008). Although the acutely-stressed *E. coli* population was then allowed to grow stress-free for an extended period of time, it was enriched for fraction of cells with longer dormancy (i.e. bacterial lag time) and higher persister frequency under ampicillin treatment. This phenomenon also appeared when *E. coli* was challenged with various stress types, suggesting the universal impact of acute stress.

In all stressed conditions, Kaplan et al. (2021) also discovered that the duration of the acute stress correlates with the tail fraction of the lag time distribution and survival fraction under ampicillin treatment. Interestingly, when SHX was added gradually into the medium instead, no heightened persister frequency nor increased heterogeneity in lag time was observed, suggesting that the stress acuteness was essential to the antibiotic persistence.

To understand the differential effect on bacteria between acutely- and gradually-applied stress, Kaplan et al. (2021) represented the bacterial cellular network (consisting of interactions among molecules such as RNAs, proteins, and metabolites) using a randomly connected cycles network model. In this network model, each node denotes a type of molecule and has two states "ON" and "OFF" to represent, say, whether the enzyme acting upon it was metabolically active for catalysis and push downstream reactions to happen. And the edge between each pair of nodes describes the interaction direction (sign) and strength (value) between them. As shown in the paper, the topology of the cellular network was sufficient to demonstrate that acute stress stochastically brings the cellular network of some cells to a disrupted regime with many molecular states turned to "OFF" mode. Once in this disrupted regime, the bacterial metabolism cannot self-regulate certain compounds to allow for quick stress recovery because other compounds are lacking, leading to a globally dysregulated state. For cells in this disrupted regime, it took a very long time for the states of all nodes to return to their original forms, resulting in an elongated lag time in a great fraction of cells. Interestingly, the fraction of cells with the lengthened lag time was associated with the duration of the acute stress exposure.

In comparison, gradual stress allows for resilience in the cellular network. The network was able to remain in a "regulated regime," where the regulatory network can maintain homeostasis in bacteria and quickly switch the "OFF" back to the "ON" mode. Together, Kaplan et al. (2021) showed that the return of the disrupted regime in the

bacteria cellular networks to their original state demonstrated a universal **physical aging** property in physical systems. By definition, physical aging says that the relaxation process of a physical system from a perturbation depends not only on the state of the system at the end of the perturbation, but also on the duration of the perturbation (Bouchaud, 1992)—in contrast to biological aging (Akermann et al., 2007). This physical aging process appeared experimentally as the duration of acute stress exposure explained persister frequency in *E. coli.*

Despite these detailed characterizations of the molecular and biophysical mechanisms behind antibiotic persistence, our knowledge on persister formation mostly came from studying single bacterial species (especially *E. coli*) in shaken test tubes. We lack understanding on how microbial ecology—relationships among microorganisms and between microbes and their physical environment—plays a role in antibiotic persistence. We need to fill this knowledge gap because bacteria almost always dwell in complex microbial communities with other bacteria species (Ratzke et al., 2020), and so it is important to consider the ecology. Therefore, a top question to answer is how antibiotic persistence relates to (1) ecological interactions among bacterial species and (2) the spatial structure of the microbial community.

I.3. Knowledge Gap: How Microbial Ecology Contributes to Persistence

I.3.1. How Positive Interspecies Interactions Contribute to Antibiotic Persistence

Interspecies interactions in bacteria are common. Bacteria often live in complex ecological communities with other species, such as within the human gut (Human

Microbiome Project Consortium, 2012) and in natural environments like soil (Weller et al., 2002) and environmental waterbody (Zimmer-Faust et al., 2021). Common pairwise, interspecies, ecological interactions within these communities include competition (-,-), commensalism (+,0), mutualism (+,+), parasitism (+,-), and predation (+,-)[1]. While positive interactions ("+" sign) are present in all but one interaction types above, they are previously considered to be rare (Foster & Bell, 2012). Experimental evidence pointed out that negative interactions such as competition dominate all types of interactions (Ghoul & Mitri, 2016; Foster & Bell, 2012). However, it was recently found that positive interactions are more common than we previously thought (Kehe et al., 2021). In fact, >50% of all pairwise cocultures of culturable soil bacteria included at least one positive interaction, by, say, increasing the growth yield of the beneficiary. Such positive interactions are indeed clinically relevant in polymicrobial infections. For example, *Pseudomonas aeruginosa* infections in Cystic Fibrosis patients rely on nutrients produced by mucin-degrading microbes in the patient lung (Flynn et al., 2016). Despite the prevalence of positive interactions, how they affect antibiotic tolerance and persistence still remains a huge knowledge gap.

One major type of positive interaction is the cross-feeding mutualism due to common auxotrophy in microbial communities. **Auxotrophy** occurs when microbes lack essential biosynthetic pathways and have to feed on certain nutrient in the environment in order to survive (Zengler & Zaramela, 2018). Auxotrophy occurs at high frequencies in

[1] Each pair-wise ecological interaction can be represented by two signs within a pair of parenthesis (__, __); each sign indicates how the presence of one species affects the other. Positive effect is shown as "+"; negative effect is indicated by "-"; and the neutral effect is represented by "0".

naturally occurring microbial communities and is crucial for community assembly and function (Zengler & Zaramela, 2018). A recent analysis of data from the Earth Microbiome Project showed that amino acid biosynthesis-related auxotrophies frequently appear in all microbial communities, especially in host-associated ones (Yu et al., 2022). The auxotrophic species in microbial communities can benefit nutrient from **cross-feeding**, where the metabolic byproducts of one species become resource for others (Fritts et al., 2021). Previous work also showed that byproduct secretion by one species allows for the evolution of a bidirectional cross-feeding (Harcombe, 2010; Harcombe et al., 2018), and such bidirectional positive interactions are defined as **mutualism** (Bronstein, 2015). Microbial species in cross-feeding communities are metabolically interdependent on one another and so a basal level of species diversity can be maintained even at low nutrient diversity (Dal Bello et al., 2021).

Previously, positive interactions were shown to shape antibiotic susceptibility in microbial communities. For one, de Vos et al. (2017) measured the antimicrobial resistance (AMR) of microbial communities in polymicrobial urinary tract infection (UTI) sites in elderly patients. The authors found that while competition was enriched in the microbial community in antibiotic-free conditions, the AMR was higher when microbes were grown in coculture with other species than grown in monoculture. These data implied the existence of a cross-protection phenotype, where the presence of community members tends to protect other isolates from antibiotics (Yurtsev et al. 2016).

On the other hand, Adamowicz et al. (2018) directly tested how metabolic

interdependency in cross-feeding communities affects AMR. Using a previously engineered cross-feeding mutualism among the *Escherichia coli*, *Salmonella enterica*, and *Methylobacterium extorquens* bacteria, Adamowicz et al. (2018) showed that the most resistant species in monoculture becomes inhibited in cross-feeding cocultures at significantly lower antibiotic concentrations. This study supported the "weakest link" hypothesis that the species least resistant in monoculture sets the resistance level in cross-feeding coculture, and also raised questions on what principles apply to antibiotic persistence. Is it possible that the "weakest link" hypothesis should be rephrased to mean that the species with the longest lag time determines the community-wide antibiotic tolerance or persistence? It is possible that metabolic interdependency can lead to higher persisters through the "persistence-by-lag" mechanism (Fridman et al., 2014).

Compared with AMR, even less is known about how interspecies interactions affect antibiotic tolerance or persistence. Here, my definitions for tolerance and persistence focus on the susceptibility of bacteria to antibiotic killing, which is different from many existing research pieces (e.g. Adamowicz et al., 2018; de Vos et al., 2017; Yu et al., 2022). These researchers used a different definition for "tolerance" as the ability of bacteria to *grow* in antibiotics in microbial community settings, which I defined as "resistance."

Interestingly, one research piece actually studied how positive interactions affected antibiotic tolerance as the population-wide killing susceptibility (Aranda-Diaz et al., 2020). The authors examined the interactions among the gut microbiome isolates from laboratory *Drosophila melanogaster*, and measured the antibiotic tolerance of a gut

Lactobacillus plantarum species against rifampin in the presence and absence of another species, *Acetobacter pasteurianus*. Aranda-Diaz et al. found that coculturing with *A. pasteurianus* greatly increased *L. plantarum's* tolerance against high-concentration rifampin. The authors found an *A. pasteurianus*-mediated increase in medium pH, which alone was sufficient for the increased *L. plantarum* tolerance. In antibiotic-free medium, the presence of *A. pasteurianus* caused a higher final growth yield in *L. plantarum*, indicating that *L. plantarum* experiences a positive interaction from *A. pasteurianus*. This study suggested that positive interactions can shape population-wide tolerance by modifying the chemical environment of the growth medium. However, whether this phenomenon was universal and how this effect of positive interactions may change antibiotic persistence remained unanswered.

I.3.2. How Spatial Structure Contributes to Antibiotic Persistence

Although microbes frequently live in microbial communities with spatial structure, microbial ecology studies usually do not consider this spatial organization (Connell et al., 2014). **Spatial structure** (aka spatial organization) is the spatial and physical distribution of bacteria in an environment. Most laboratory experiments are conducted in shaken test tubes, where bacteria are considered to be planktonic. In shaken tubes, the entire volume of the growth medium is considered to be spatially homogeneous and to have no spatial structure. But spatial structure is important in natural microbial communities as bacteria can dwell *in vivo* in small, packed aggregates, which then modulate physiology (Connell et al., 2014).

Recently, the importance of spatial structure has been studied in terms of growth heterogeneity of individual bacterial colonies in a single species, *E. coli* or *S. enterica* (Chacón et al., 2018). Using time-lapsed imaging of agar plates spread with *E. coli* or *S. enterica*, Chacón et al. found that final colony sizes within monoculture of bacteria are best predicted by territoriality. These results make one wonder whether the effect of metabolic interdependency on growth will become more spatially explicit between cross-feeding partners on coculture agar. Together, how spatial structure and the cross-feeding interactions between bacterial species affect antibiotic tolerance or persistence remains an open question.

Previous work prepared preliminary results to help answer the aforementioned open question. Dal Co et al. (2019) created a glucose gradient on lawn of isogenic *E. coli* cells within a microfluidic chamber, and found evidence for cross-feeding between glucose-fermenting and acetate-respiring subpopulations of *E. coli*. When challenged with a lethal antibiotic pulse, higher survival was found in the microfluidic chamber than in shaken conditions. Together, these results suggested the protective effect of spatial structure against antibiotic pulses. More recently, Dal Co et al. (2020) engineered a pair of amino acid cross-feeding *E. coli* strains and studied their ecology in the microfluidic chamber. The authors found that the growth rates of single-cell *E. coli* was best explained by the fraction of the cross-feeding partner within a small neighborhood.

Despite these studies, much remained unanswered about the effect of spatial structure and cross-feeding on antibiotic tolerance and persistence. In Dal Co et al.

(2019), it was unknown whether the glucose gradient was sufficient to cause differential survival fractions by antibiotic killing. Answering this question will help disentangle the effect of cross-feeding from the glucose gradient. Second, whether the higher antibiotic survival in microfluidic chambers was due to antibiotic tolerance or persistence has not been investigated either, which made it difficult to understand the detailed mechanism. In conclusion, while previous work was related to the open question above, how spatial structure and cross-feeding together affect antibiotic persistence has not been studied in detail.

I.4. Overview of Thesis Work

In this thesis, I used wet-lab experiments and mathematical models to study how antibiotic persistence was regulated by spatial structure within a cross-feeding microbial mutualism. Shown in Fig. 1.3a, this synthetic obligate mutualism was previously evolved between an *E. coli* and a *Salmonella enterica* strain that cross-feed each other on a minimum agar with lactose as the only carbon source (Harcombe, 2010; Harcombe et al., 2014). Specifically, the *E. coli* strain is a methionine-auxotroph and feeds on the methionine secreted by the *S. enterica* strain and on lactose in the environment. *S. enterica* feeds on *E. coli*'s acetate secretion. And both strains feed on ammonia in the environment. To ensure spatial structure, I randomly distributed bacterial cells (both in monoculture and in mutualistic coculture) on a filter membrane (Fig. 1.3b), which was then transferred between agar plates with different chemical composition. This experimental setup was the cornerstone to my thesis work.

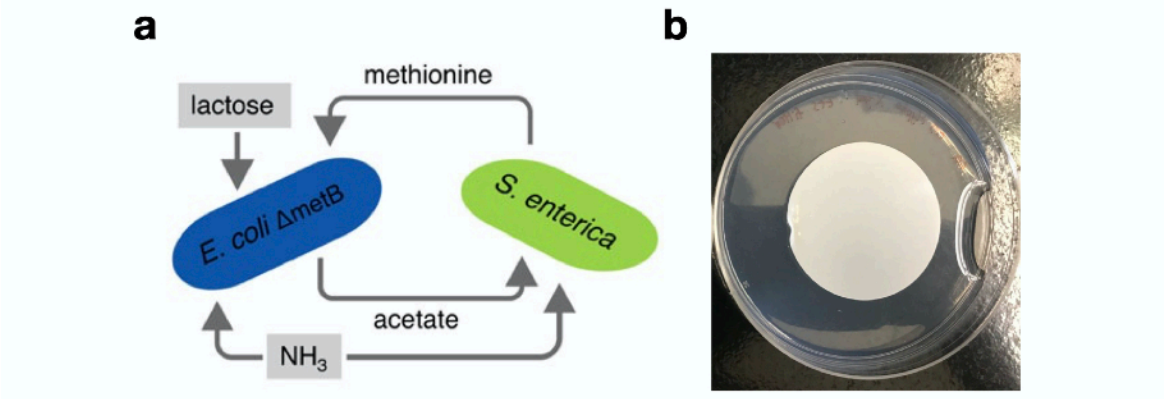

Figure 1.3. Research Framework of My Thesis. a A previously-evolved synthetic cross-feeding *E. coli* and *S. enterica* community was used as the model ecological community in this thesis. Figure 1a in Hammarlund et al. (2019) was reproduced here. **b** A filter membrane with appropriate *E. coli* and/or *S. enterica* on it was placed onto a minimum agar with lactose as the only carbon source. This filter could be moved to new agar media with different nutrient compositions.

As a result, I discovered that in the presence of spatial structure, the persister frequency of *E. coli* is ~100-fold higher when it is cross-feeding with *S. enterica* than when *E. coli* is grown alone. Interestingly, antibiotic tolerance was not affected. Subsequently, I performed analysis on the growth physiology at a single-colony resolution for *E. coli* grown on agar surfaces, and used this analysis to reveal the mechanism behind the heightened persistence level in the cross-feeding coculture. Finally, I designed a partial differential equation (PDE) based mathematical model to attribute the increased persister frequency to the spatial heterogeneity of methionine distribution, which leads to larger variance in single-cell growth rate and duration of the lag phase.

CHAPTER II: RESEARCH APPROACH & METHODS

II.1. Experimental Approach

II.1.1. Bacterial Strains & Media

Bacterial Strains: To mechanistically investigate whether cross-feeding mutualisms affect persister frequency, I used a pair of previously domesticated bacterial species, *Escherichia coli* and *Salmonella enterica*. The *E. coli* K-12 (BW25113) used was a Δ*metB* strain from the Keio collection and has an hfr line to insert the lac operon (labeled as WRH221; Baba et al., 2006). The *S. enterica* LT2 strain used was a mutant selected and engineered to secrete methionine (labeled as WRH201; Harcombe, 2010). Both *E. coli* and *S. enterica* are labeled with fluorescents proteins by transducing genes encoding them under constitutive promoters. Respectively, *E. coli* strain WRH224 is labeled with the cyan fluorescent protein (CFP) and *S. enterica* strain WRH240 is labeled with yellow fluorescent protein (YFP).

Hypho Minimum Medium/Agar: To ensure that *E. coli* and *S. enterica* engage in various ecological interactions, I used the Hypho minimum medium containing phosphate, nitrogen, sulphate, and various carbon sources as previously described (Harcombe et al., 2014). As shown in Fig. 1.4a, *E. coli* and *S. enterica* engage in mutualism by cross-feeding to each other acetate and methionine, respectively. So the mutualistic coculture medium contains 2.78 mM lactose as the sole carbon source. To supplement the auxotrophic *E. coli* with methionine, the *E. coli* monoculture medium contains 2.78 mM lactose and 0.08 mM methionine. The *S. enterica* monoculture medium contains16.9 mM acetate as the sole carbon source. For *E. coli* to be in a

commensalism with *S. enterica* with *S. enterica* being the beneficiary, the *E. coli* monoculture medium was used with both *E. coli* and *S. enterica* present. Finally, the competition medium between *E. coli* and *S. enterica* contains 0.08 mM methionine and 0.056 mM glucose. When appropriate, Hypho minimum agar was prepared by adding 1% (g/mL) of agar powder to water to be autoclaved. Afterwards, filter-sterilized carbon source, salts, and ampicillin were added.

LB agar: LB agar was made for enumeration of cell density (see Section II.1.3). LB agar was made by adding 1 L DDI (distilled and deionized) water with 10 g agar, 10 g NaCl powder, 5 g yeast extract, and 10 g tryptone powder prior to autoclave sterilization. X-gal was added into the post-autoclave LB agar medium for distinguish between the lactose-metabolizing *E. coli* (blue colonies) and the *S. enterica* strain that does not metabolize on lactose (white colonies).

II.1.2. Tracking Bacteria in A Spatially-Structured Environment

By fixing *E. coli* and/or *S. enterica* onto nitrocellulose membrane (Fig. 2.1), I created a spatially-structured environment for bacteria that can be transferred between

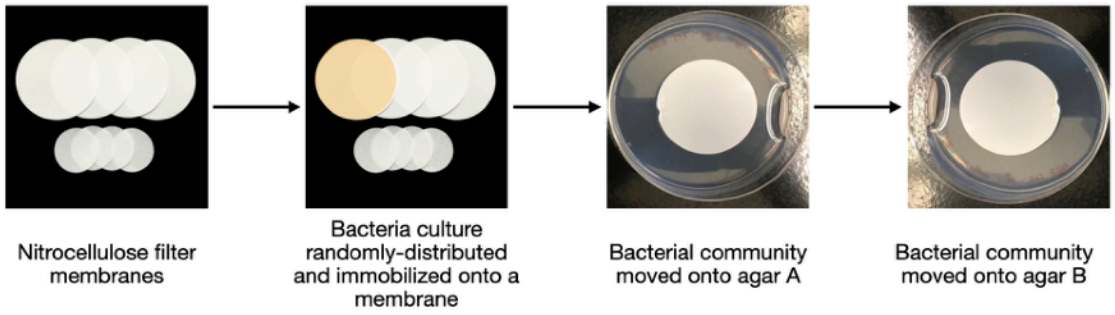

Figure 2.1. Creating a Spatially-Structured Environment for Bacteria. Overnight bacterial culture was added onto a nitrocellulose membrane (shown in orange) and air-vacuumed to move the liquid medium. The bacterial population/community was then fixed onto the membrane, and can be moved between agar plates A and B with various medium composition to be assessed for bacterial behavior.

agar with different medium compositions. *E. coli* and/or *S. enterica* culture was cultivated overnight in appropriate Hypho minimum media. 2 mL of OD=0.005 diluted culture was overlaid onto a nitrocellulose membrane (Radius: 4.7 mm; Thermo Fisher Scientific, MA) and then air-vacuumed to remove the liquid medium. The bacterial population/ community was then fixed onto the membrane, and the membrane can be moved between agar plates with different medium composition (Fig. 2.1).

II.1.3. Antibiotic Tolerance & Persistence Assays

Antibiotic tolerance and persistence were measured as in Fridman et al. (2014) and Balaban et al. (2019). *E. coli* and *S. enterica* were grown overnight respectively in liquid Hypho minimal media at 37^{o}C to log phase (OD_{600} ~ 0.2; from now on OD_{600} is referred to as "OD") and then seeded into fresh liquid medium or nitrocellulose membranes to acquire survival curves measured by survival fraction over time. The experimental protocols for measuring antibiotic tolerance and persistence are described below. All experiments were done in 3~6 biological replicates.

Survival Curve Experiment in Liquid: *E. coli* and *S. enterica* cells were seeded into 10 mL fresh Hypho medium with appropriate nutrient supplementation. The seeding concentration for *E. coli* or *S. enterica* monoculture was OD = 0.01 per mL, and was OD = 0.005 per mL per species in the mutualistic coculture. The fresh culture was then incubated at 37 ^{o}C or 30 ^{o}C with shaking for 1 h. To initiate the killing experiment, ampicillin (Fisher Scientific, MA) was then added at 100 μg/mL (Balaban et al., 2004), and the culture was incubated at the same temperature as the pre-treatment incubation

with shaking for 24 h. Right before adding ampicillin and during ampicillin killing, culture were sampled by taking 100 μL for CFU (colony forming unit) counting and the subsequent tolerance and persistence calculation.

Survival Curve Experiment with Spatial Structure: *E. coli* and *S. enterica* cells were first seeded into saline solutions, where the saline stress was known not to cause increased persistence (Kaplan et al., 2021). In monoculture, *E. coli* and *S. enterica* were seeded at OD = 0.005 per mL saline. In the mutualistic coculture, *E. coli* and *S. enterica* were seeded at OD = 0.0035 and OD = 0.0025 per mL, respectively. An amount of 2 mL of the bacteria in saline was added onto a fresh nitrocellulose membrane and air-vacuumed to remove all liquid medium. The membrane was incubated on a fresh Hypho minimum agar for 2 h at 37 ^{o}C or 30 ^{o}C, before moving onto a new Hypho agar with 100 μg/mL ampicillin. The agar was then incubated for various durations up to 24 h at the same temperature as the pre-treatment incubation. Every time the survival rate needs to be assessed, the membrane on an agar plate was sacrificed to be vortex-washed for 30 s in 10 mL of saline, which was then serially diluted and used to calculate antibiotic tolerance and persistence.

Serial Dilution & Antibiotic Tolerance/Persistence Calculation: The ampicillin culture sampled at each killing duration of the killing experiment (i.e. the 100 μL samples from the liquid experiment or the 10 mL bacterial saline solution from the agar experiment) was used to perform serial dilutions in saline solutions. A stock solution of 5000 unit/mL of beta-lactamase was made in sterile water and kept at 4 ^{o}C (Neta

Scientific, NJ) as in Balaban et al. (2004), and this stock was diluted at a 1:40 ratio to saline solutions for serial dilutions to up 10^{-4}. A volume of 75 uL of each dilution was spread on a fresh LB agar with X-gal for a 24 h incubation in 37 ^{o}C and for a subsequent 5-day incubation at room temperature (~24^{o}C). This long incubation process was to ensure that all colonies—including the small colony variants—appear to form visible colonies (Vulin et al., 2018). CFU was calculated and used to calculate survival rate at each killing duration against the CFU immediately before killing (i.e. 0 h).

The survival curve was then used to calculate antibiotic tolerance, persistence, and the persister fraction. Tolerance (MDK_{99}) and persistence ($MDK_{99.99}$) were measured using the survival curve for each biological replicate and strain to identify the time it takes to kill 99% and 99.99% of the population, respectively. To calculate the persister fraction, I fit an exponential curve to the less steep phase of the biphasic kill curve, and the interaction between this exponential curve with the *y*-axis was considered persister fraction (Balaban et al., 2019).

II.1.4. Population-Level Bacterial Growth Physiology Assays

The growth physiology was measured for *E. coli* and *S. enterica* bacteria grown in Hypho minimal media—both in monoculture and in mutualistic coculture. Measurement in liquid and on agar plates are described separately.

Growth in Liquid: Growth in liquid was measured as the population-level growth rate of *E. coli* and *S. enterica* in a a given liquid medium. I collected fluorescence signals of the constitutively expressed CFP in *E. coli* and YFP in *S. enterica* in each bacterial

population/community. Fluorescence signals were measured to indicate growth instead of OD so that growth of each species can be simply measured in mutualistic coculture of *E. coli* and *S. enterica*. The two species, *E. coli* and *S. enterica*, were grown overnight in liquid Hypho minimum media at 37^{o}C to log phase (OD ~ 0.2) and then seeded into 200 μL fresh liquid medium in a 96-well plate at OD = 0.005 per mL. The fluorescent signal is read using a microplate reader (TECAN Tradings, Switzerland) every 20 min for ~ 250 cycles with continuous shaking at 37 ^{o}C or 30 ^{o}C. Fluorescence of CFP (YFP) is collected at excitation wavelength 430 (500) nm and emission wavelength 490 (530) nm. The growth rate in each well was calculated by fitting a Baranyi function to the population growth curve using an in-house code (Baranyi & Roberts, 1994).

Growth on Nitrocellulose Membranes: *E. coli* and *S. enterica* were grown overnight in liquid Hypho minimum media at 37^{o}C to log phase (OD_{600} ~ 0.2; from now on OD_{600} is referred to as "OD") and then seeded onto nitrocellulose membranes as in Section II.1.3., which were then placed on a Hypho minimum agar without antibiotics. The agar plate was incubated for 0 h, 1 h, and 2 h at 37 ^{o}C before CFU counting and growth curve plotting. Similar procedure was followed as in Section II.1.3, where an entire nitrocellulose membrane is sacrificed to calculate CFU at each harvesting time point.

Measurement of Indole Production in *E. coli*: The production of indole in *E. coli* was measured on nitrocellulose membranes placed on Hypho agar in either monoculture or coculture with *S. enterica*. At time points of measurement, the membrane and the

volume of the agar directly covered by it were taken up and vortexed in 10 mL DDI water for 30 s. Then the measurement followed protocols in in Darkoh et al. (2015). Briefly, fresh indole standards ranging from 0 to 300 μM were prepared in 70% ethanol. In a new 2-mL eppendorf tube, indole standards or the vortexed *E. coli* sample in a volume of 300 μL were incubated for 15 min at room temperature with 75 μL of 5.3 M NaOH and 150 μL of 0.3 M NH_2OH-HCl. Following incubation, a volume of 375 μL of 2.7 M H_2SO_4 was added, vortexed, and incubated at room temperature for another 30 min to yield a pink solution that was measured spectrophotometrically at a wavelength of 530 nm. Because *E. coli* was indole-positive and *S. enterica* is indole-negative, the same protocol can be used for *E. coli* in mono- or co-culture.

II.1.5. Single-Colony Level Bacterial Growth Assay

Time-Lapsed Imaging for *E. coli* Growth: Individual *E. coli* may exhibit various growth phenotypes (Kiviet et al., 2014). While this phenotypic heterogeneity needs to be studied thoroughly, the above techniques in Sections II.1.4 cannot achieve this task. Here, I performed a high-throughput quantification of *E. coli* growth physiology by examining each *E. coli* colony's growth rate and lag time when plated on Hypho minimal agar as in Chacón et al. (2018). The single-colony *E. coli* growth physiology was known to approximate single-cell growth (Levin-Reisman et al., 2010). Briefly, a total of 100~200 *E. coli* and/or *S. enterica* cells were spread on appropriate Hypho agar and subjected to time-lapsed imaging at 37 ^{o}C or 30 ^{o}C over a course of 10~14 days. In time-lapsed imaging, an Epson Perfection V600 Photo office scanner (Epson America Inc, CA) was

programed to take an image of the agar plate once per hour, and the growth rate and appearance time of each individual colony were measured using in-house programs for image analysis and data analysis. The programs were built to achieve similar functions as in Levin-Reisman et al. (2010) and Chacón et al. (2018).

Image & Data Analysis: The area size (unit: pixels) of each individual colony on the agar plate was calculated using an in-house Python code by Dr. Jeremy Chacón, a Research Associate in the laboratory. Briefly, *E. coli* and *S. enterica* were distinguished using the natural coloration differences between the two species, and the unsupervised learning technique was used to classify the species of each colony. The computer-classified species of each colony was then manually curated by examining the coloration and colony morphology of disputable individual colonies under a stereoscope. If necessary, the disputable colony was spread on a separate LB agar with X-gal to observe the coloration as in Section II.1.3.

The data of colony area size over incubation time were further analyzed using my custom-built code. Appearance time of individual colonies were recorded as the earliest incubation duration at which the colony area becomes non-zero, similar to the practice in Levin-Reisman et al. (2010). The growth rate was calculated by first converting the colony area data into radius data, and then applying a linear line to the initial growth phase of the colony, which is defined to be between the colony appearance time and the time it takes to reach half of the maximum radius size in the stationary phase.

II.2. PDE-Based Mathematical Model

II.2.1. Overview of the Mathematical Model

To understand how spatial structure relates to the observed differences in *E. coli* antibiotic persistence, I developed a mathematical model using partial differential equations (PDEs) to computationally simulate growth of individual *E. coli* and *S. enterica* colonies in monoculture and mutualistic coculture on a 1D line.

In the resource-explicit model I built, bacterial colonies interact with local nutrients in a spatially-structured environment to grow. On a 1-dimension line of distance $Y = 5$, individual cells of *E. coli* (*E*) and/or *S. enterica* (*S*) were seeded randomly by setting the initial conditions at $t = 0$ to be non-zero at random locations, *x*, whereas various nutrients were initially overlaid evenly on the entire line. This random seeding of bacterial cells makes the PDE model able to describe bacterial populations and communities with spatial structure. Each PDE in Equations [1~2] denote the rules regarding how abundance of bacteria or nutrients changes over 40 units of time, $t \in [0,40]$, at any particular *x*.

Equations in [1] denote how *E. coli* and *S. enterica* cross-feed and grow in a mutualistic community. First, the growth of *E. coli* and *S. enterica* follow Eq. [1a] and [1b], respectively. *E. coli* grows by consuming methionine (*M*) and lactose (*L*), whereas *S. enterica* grows by taking in acetate (*A*). The maximum growth rates are r_E and r_S, respectively, and the instantaneous growth rates are limited by the nutrient's local concentration in a Monod fashion with the half-saturation constants, K_M, K_L, and K_A.

Growth is ultimately limited by exhaustion of nutrient explained below. *E. coli* growth rates depend on both methionine and lactose, while *S. enterica* growth rates depend only on acetate (see Section II.2.2 for Model Assumptions).

$$\frac{\partial E}{\partial t} = r_E \left(\frac{M}{M + K_M} \right) \left(\frac{L}{L + K_L} \right) E - \kappa_E E, \quad [1a]$$

$$\frac{\partial S}{\partial t} = r_S \left(\frac{A}{A + K_A} \right) S - \kappa_S S. \quad [1b]$$

Eq. [1c] denotes the temporal dynamics of methionine. As a nutrient source, methionine diffuses in space over time at a rate, D_M. It is produced by *S. enterica* at a rate, p_M, and is proportional to *S. enterica*'s consumption of acetate in a Monod fashion (Hammarlund et al., 2021). In another word, *S. enterica* only produces methionine when metabolizing on acetate. Methionine gets consumed by *E. coli* following a Monod kinetics by a maximum rate, c_E. Finally, methionine degrades slowly over time at a rate, κ_M.

$$\frac{\partial M}{\partial t} = D_M \nabla^2 M + p_M r_S \left(\frac{A}{A + K_A} \right) S - c_E \left(\frac{M}{M + K_M} \right) \left(\frac{L}{L + K_L} \right) E - \kappa_M M. \quad [1c]$$

Similar to methionine, acetate diffuses at a rate, D_A, gets consumed by *S. enterica* following Monod kinetics, decays exponentially by κ_A (Eq. [1d]). Note that acetate is produced by *E. coli* at a rate, p_A, as both lactose and methionine are being consumed. Acetate concentration decreases due to *S. enterica* consumption by a maximum rate, c_S.

$$\frac{\partial A}{\partial t} = D_A \nabla^2 A + p_A r_E \left(\frac{M}{M + K_M} \right) \left(\frac{L}{L + K_L} \right) E - c_S \left(\frac{A}{A + K_A} \right) S - \kappa_A A. \quad [1d]$$

Finally, the temporal dynamics of lactose concentration—which is only consumed by *E.*

coli—follows Eq. [1e]. Here, the natural decay rate of lactose is, κ_L.

$$\frac{\partial L}{\partial t} = D_L \nabla^2 L - c_L \left(\frac{M}{M + K_M} \right) \left(\frac{L}{L + K_L} \right) E - \kappa_L L. \quad [1e]$$

The Neumann boundary conditions are:

$$\frac{\partial N}{\partial x} = 0 \text{ at } x = 0,\ 5, \quad [1f]$$

for $N \in \{E, S, M, A, L\}$.

To simulate *E. coli* grown in monoculture, we remove *S. enterica*- and acetate-associated terms from Eqs. [1] to form Eqs. [2] below, as methionine and lactose are now supplemented in the growth medium for monoculture *E. coli* and so no production terms are necessary. All variables are identical to those in Eqs. [1].

$$\frac{\partial M}{\partial t} = D_M \nabla^2 M - c_E \left(\frac{M}{M + K_M} \right) \left(\frac{L}{L + K_L} \right) E - \kappa_M M, \quad [2a]$$

$$\frac{\partial E}{\partial t} = r_E \left(\frac{M}{M + K_M} \right) \left(\frac{L}{L + K_L} \right) E - \kappa_E E, \quad [2b]$$

$$\frac{\partial L}{\partial t} = D_L \nabla^2 L - c_L \left(\frac{M}{M + K_M} \right) \left(\frac{L}{L + K_L} \right) E - \kappa_L L. \quad [2c]$$

Similarly, the boundary conditions are:

$$\frac{\partial N}{\partial x} = 0 \text{ at } x = 0,\ 5. \quad [2d]$$

for $N \in \{E, M, L\}$.

II.2.2. Model Assumptions

My simple PDE models above are based on the following assumptions.

1. Bacterial growth can be achieved by only consuming among 3 types of nutrients (methionine, lactose, and acetate). In reality (experiments), more nutrients sources have to be present to support growth. For example, ammonia is present in the medium for both monoculture and mutualistic coculture. Thus, the impact of ammonia concentration on growth was factored into the growth rate variables r_E and r_S.
2. The only interaction between *E. coli* and *S. enterica* in the mutualistic coculture is the cross-feeding of methionine and acetate. This may deviate from reality because experimental RNA-Seq data suggest that *E. coli* may also produce galactose for *S. enterica* to consume (Unpublished data; Previous indications in Harcombe et al., 2018).
3. Nutrient production of both *E. coli* and *S. enterica* only occurs when their growth nutrients are present. In reality, *E. coli* initiates the mutualism by producing acetate without having to metabolize on methionine (Unpublished data). This assumption allows me to keep the model simple without having to make special mathematical treatment for *E. coli*. The issue is further discussed in the Model Implementation & Parametrization section (Section II.2.3).
4. Bacterial growth leads to no diffusion of biomass. In reality, bacterial growth on agar surfaces results in colony formation and colony size expansion (Chacón et al., 2018). This can change the average distance among bacterial colonies. Because my research only considers how the initial distribution of bacterial cells

determines spatial structure, I incorporated this assumption in my model for simplicity.

5. The growth rate of each colony reflects the instantaneous growth rate of individual cells on the nitrocellulose membrane before ampicillin treatment in the experiment.
6. Bacteria naturally die and nutrients naturally decay over the course of the modeling. These decays are linear with respect to the instantaneous abundance of the bacteria or the nutrient.
7. The resource-explicit growth of *E. coli* is based on the product of the two Monod terms, and not the minimum of the two as in Hammarlund et al. (2019).

II.2.3. Model Implementation & Parameterization

To compare the growth physiology of *E. coli* in cross-feeding coculture (Eq. [1]) and in monoculture (Eq. [2]), I performed nondimensionalization for both sets of equations to make all variables unit- and dimension-less (See details in Appendix II: Supplementary Mathematical Analysis). Twenty locations on the 1D line were selected randomly to seed *E. coli* (and *S. enterica*, if in the mutualistic coculture) biomass at the initial time points, when nutrient was distributed evenly on the line as well. Then, I numerically solved Eq. [1~2] in MATLAB R2021b with the pdepe function. Finally, I calculated the growth rates and lag time of individual colonies by fitting a log-linear growth curve to the log-transformed biomass. These results were then used to explain the antibiotic persistence data observed in experiments.

Model parameters were chosen based on the ones in the dimensionless ODE (ordinary differential equations) model in Hammarlund et al. (2021) that described the growth of the same experimental system in liquid. Updates of these parameters were made to ensure that ratios between certain parameters reflect experimental measurements, and the diffusion parameters were chosen based on Chacón et al. (2018). A full parameter list can be found in Table S2 (Appendix II: Supplementary Mathematical Analysis).

Note that very little (but non-zero) abundance of methionine and acetate were seeded evenly on the 1D line in the PDE model for the cross-feeding coculture. This is a convention in cross-feeding models (e.g. Hammarlund et al., 2019; Hammarlund et al., 2021) to allow the PDE system to produce dynamics representative of experimental measurements.

II.3. Statistics

To understand whether observed differences in measurements between treatment groups—in both mathematical modeling and in wet-lab experiments—were statistically meaningful, I used R v.3.3.3 (R Core Team, 2016) to perform analysis of variance (ANOVA) with adjusted *p*-values using Tukey's HSD (honestly significant difference; Lee & Lee, 2018), and linear regressions as described throughout the Results chapter (Chapter III).

CHAPTER III: RESULTS

III.1. Antibiotic Persistence in A Spatially-Structured Experimental Environment

III.1.1. Antibiotic Persistence in A Spatially-Structured Environment

To understand whether cross-feeding affects antibiotic persistence in a spatially-structured environment, I fixed bacteria on surfaces of nitrocellulose membranes (Section II.1.2), and treated *E. coli* and *S. enterica* on monoculture and mutualistic coculture Hypho agar with high-concentration ampicillin at 37 ^{o}C (Fig. 3.1a). First, the kill curves of *E. coli* were biphasic in both monoculture and coculture, suggesting the presence of persisters in both ecological conditions. Surprisingly, the MDK_{99} measurements were similar between coculture and monoculture, showing similar *E. coli* antibiotic tolerance

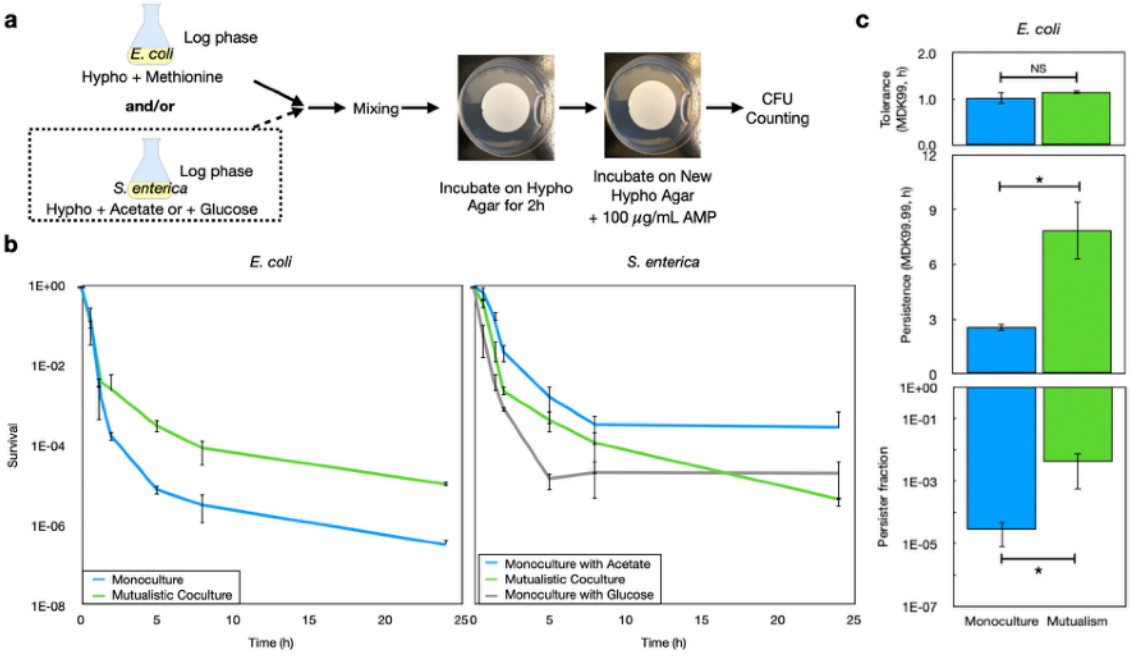

Figure 3.1. Bacterial Killing Dynamics Differs in Monoculture and in Mutualistic Coculture. a *E. coli* and *S. enterica* were grown in Hypho minimum medium till log phase, and then fixed on nitrocellulose membranes in either monoculture or in mutualistic coculture as in Section II.1.2~II.1.3 for ampicillin treatment. **b** Survival curves of the ampicillin over 24 hours were plotted. Error bars denote standard deviation of 3 biologically independent trials. **c** Antibiotic tolerance, persistence, and persister fractions of *E. coli* were calculated following the Methods chapter. NS: no significance, $p>0.05$; *: $p<0.05$.

in both monoculture and coculture (Fig. 3.1c; One-way ANOVA, p=0.237). However, survival in coculture was significantly higher than in monoculture by 5-hour ampicillin treatment (One-way ANOVA, F[1]=34.57, p=0.0042), by as much as ~40-fold. Furthermore, the $MDK_{99.99}$ measurement showed a significantly higher antibiotic persistence in mutualistic coculture (Fig. 3.1c; One-way ANOVA, p=0.000975), and this is consistent with a ~100-fold higher antibiotic persister frequency in coculture (Fig. 3.1c; One-way ANOVA, p=0.00286). Together, these results suggested higher *E. coli* persister frequency when grown in the cross-feeding coculture, but not population-wide tolerance.

In comparison, the kill curves of *S. enterica* have different features from *E. coli*. The initial killing rates of *S. enterica* in all tested ecological conditions are different. In particular, when grown in Hypho minimum media with acetate or glucose as the only carbon source, the monoculture *S. enterica* demonstrated different killing kinetics. I tested these monoculture conditions because acetate was not the only metabolite that *S. enterica* receives from *E. coli* (Harcombe et al., 2018; Adamowicz et al., 2020), and it still remains unknown what other metabolites *S. enterica* consumes during cross-feeding. Therefore, I decided to focus my effort on understanding the differential antibiotic persistence of *E. coli* during ampicillin treatment.

The data in Fig. 3.1 raised an important question of why antibiotic persistence of *E. coli* is higher in the cross-feeding coculture than in monoculture. I developed four hypotheses that could explain this observation.

- **Hypothesis 1:** The presence of *S. enterica* increases *E. coli* persistence to

antibiotics because *S. enterica* changes the chemical profile that *E. coli* experiences. This may be consistent with a previous study (Aranda-Diaz et al., 2020). In this study, the antibiotic tolerance of *Lactobacillus plantarum* in the fruit fly gut is higher when grown with *Acetobacter pasteurianus*, which changed the environmental pH and increased *L. plantarum* tolerance.

- **Hypothesis 2:** Cross-feeding alone drives the heightened antibiotic persistence in *E. coli*. Dal Co et al. (2019) showed that cross-feeding in *E. coli* grown in a microfluidic chamber led to an increased survival against antibiotic challenge. It is possible that being in a microfluidic chamber is not the preliminary cause.
- **Hypothesis 3:** *E. coli* growth rates are different between monoculture and mutualistic coculture, and this growth rate difference can explain persistence difference. This is consistent with the fact that higher growth rate of *E. coli* correlates with higher death rate by beta-lactams *in liquid* (Lee et al., 2018).
- **Hypothesis 4:** The difference in *E. coli* antibiotic persistence is specific to a spatially-structured environment. Spatial structure is known to cause heterogeneity in growth rate or growth yield in monocultures (Chacón et al., 2018). Potentially, this heterogeneity may be heightened in cross-feeding coculture compared to monoculture, because *E. coli* is metabolically dependent on *S. enterica* (Adamowicz et al., 2020).

Here, I investigated these four hypotheses separately and propose an answer to the question above.

III.1.2. The Presence of S. enterica Alone Cannot Explain Persistence Differences

In studying Hypothesis 1, I aimed to test whether the presence of *S. enterica* alone can explain the difference in antibiotic persistence of *E. coli* between mono- and co-culture at 37 ^{o}C. First, I aimed to study *E. coli*'s antibiotic response when it is grown with *S. enterica* but not metabolically dependent on it. To achieve this, I incubated our *E. coli* methionine auxotroph together with *S. enterica* on Hypho minimal agar with lactose and methionine in the same nitrocellulose membranes setting as in Section III.1.1, and compared *E. coli*'s antibiotic response with data in Section III.1.1. As shown in Fig. 3.2a, as long as methionine was present in the environment—whether it was supplemented (Monoculture; Met-Supplemented Coculture) or produced by a mutualistic partner (Cross-Feeding Coculture)—I observed little to no difference in antibiotic tolerance in *E. coli* (One-way ANOVA, F[1]=0.172, p=0.69). However, *E. coli* antibiotic persistence and persister frequency depended on how methionine is provided (One-way ANOVA,

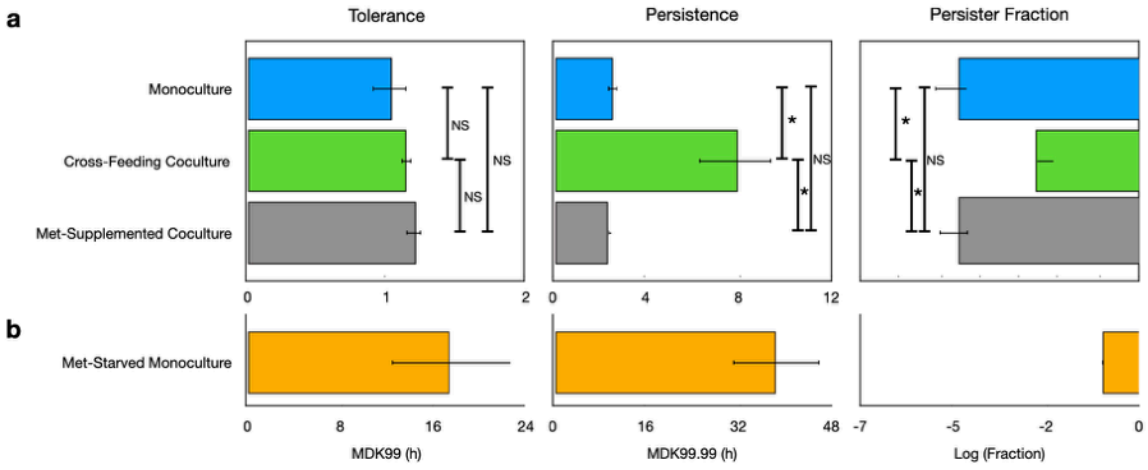

Figure 3.2. The Presence of *S. enterica* Alone Does NOT Explain the Heightened Antibiotic Persistence of *E. coli* in Coculture. Antibiotic tolerance, persistence, and persister fraction were calculated following Chapter 2 for *E. coli* at 37^{o}C. Met-Supplement Coculture: *E. coli* was incubated with *S. enterica* on Hypho agar containing lactose and methionine. Met-Starved Monoculture: *E. coli* was incubated alone on Hypho agar with only lactose and no methionine. Error bars denote standard deviation of 3 biologically independent trials. NS: no significance, p>0.05; *: p<0.05.

F[2]=26.89, p=0.00211). In particular, when methionine was externally supplemented in the agar, there was no difference in *E. coli*'s persistence measurement (One-way ANOVA, Tukey's HSD p=0.993) or persister fraction (One-way ANOVA, Tukey's HSD p=0.9998) as compared to monoculture.

In contrast, the heightened antibiotic persistence and persister fraction were only seen when *E. coli* depends on *S. enterica* to provide methionine (Fig. 3.2a). When *E. coli* metabolically depends on *S. enterica* for methionine, *E. coli* has higher persistence than when it can get methionine from the media with (One-way ANOVA, Tukey's HSD p=0.000893) or without *S. enterica* (One-way ANOVA, Tukey's HSD p=0.000975). Similarly, higher *E. coli* persister fraction was seen in the cross-feeding coculture compared to in monoculture (One-way ANOVA, Tukey's HSD p=0.00286) or on coculture agar with *S. enterica* and methionine supplementation (One-way ANOVA, Tukey's HSD p=0.00290). Together, these results suggest that the presence of *S. enterica* alone is insufficient to cause the high antibiotic persistence phenotype in *E. coli* (Fig. 3.2a), raising a hypothesis that metabolic dependency on *S. enterica* may be a key to the heightened persistence.

One possible rebuttal to the discovery above is that *E. coli* that metabolically depends on *S. enterica* are on-average starved for methionine. To test whether this rebuttal is true, I starved *E. coli* by incubating it alone on Hypho agar with lactose and **no** methionine for antibiotic killing assays (Fig. 3.2b). I found a heightened *E. coli* antibiotic tolerance in this starved condition compared with no methionine starvation, by ~12 fold

in MDK_{99} measurements. Even though much higher persistence and persister fraction were also observed, it is difficult not to associate the persistence change with tolerance change. As a result, these data point out a strong distinction between *E. coli* in coculture with *S. enterica* (persistence change only) and *E. coli* in the methionine-starved condition (tolerance change as well; Fig. 3.2b).

All of the results in Section III.1.2—and in Fig. S1 (Appendix III: Supplementary Result Figures)—together conclusively showed that the presence of *S. enterica* alone does not explain the heightened *E. coli* antibiotic persistence in the cross-feeding coculture. Therefore, Hypothesis 1 has been falsified.

III.1.3. Cross-Feeding Alone Cannot Explain Antibiotic Persistence Differences

Next, I tested whether cross-feeding with *S. enterica* is sufficient to explain the difference in *E. coli*'s antibiotic persistence (Hypothesis 2). Results in Section III.1.2 show that the presence of *S. enterica* does not increase persistence for *E. coli*, but we still do not know whether acquiring methionine from *S. enterica* (i.e. metabolic dependency on *S. enterica*) suffices to increase *E. coli* persistence. To test this, I repeated the antibiotic killing assays for *E. coli* but in liquid Hypho minimum media (Fig. 3.3a). No observable differences in *E. coli* kill curves were seen between mono- and co-culture (Fig. 3.3b). The measurements for antibiotic tolerance (One-way ANOVA, p=0.9327) and persistence (One-way ANOVA, p=0.5137) were not different between the two conditions either. Data here are consistent with those in Fig. 3.2a because both ruled out the possibility that other unknown metabolites that *E. coli* receives from cross-feeding can

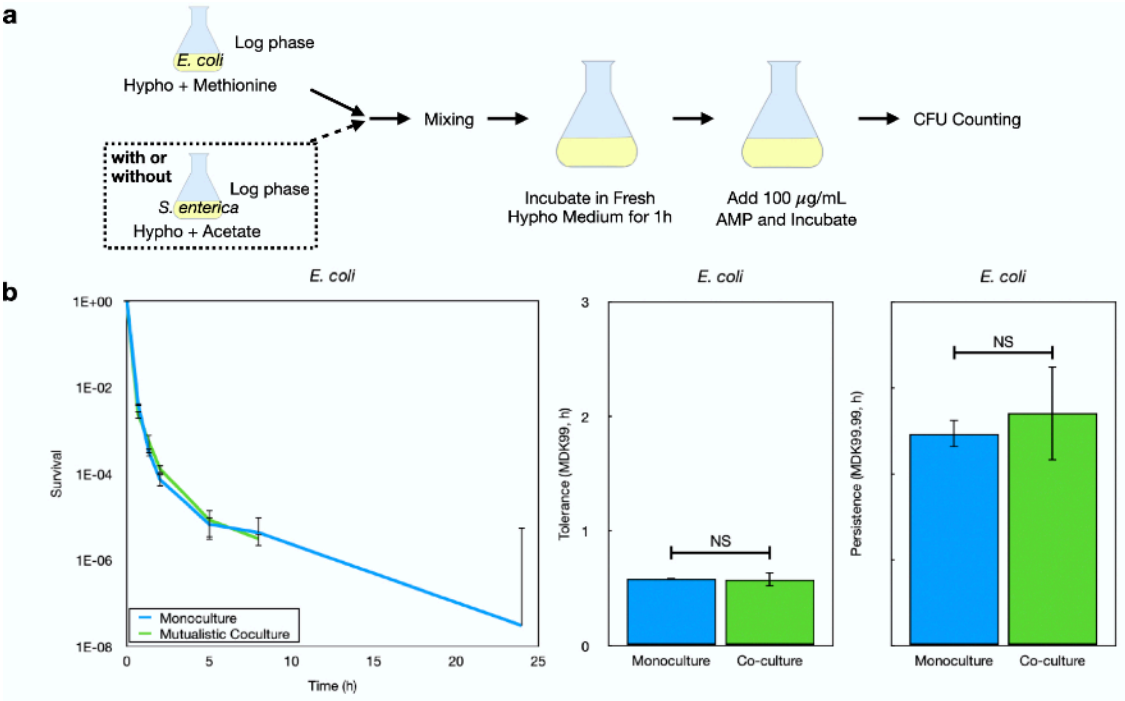

Figure 3.3. In Liquid, *E. coli*'s Killing Dynamics is Similar in Monoculture and in Mutualistic Coculture. a *E. coli* and *S. enterica* were grown in Hypho minimum medium till log phase, and then diluted in fresh Hypho minimum medium in either monoculture or in mutualistic coculture as in Section II.1.2~II.1.3 for ampicillin treatment. **b** Survival curves of the ampicillin over 24 hours were plotted, and antibiotic tolerance and persistence were measured by MDK99 and MDK99.99, respectively as described in Chapter 2. Error bars denote standard deviation of 3 biologically independent trials. NS: no significance, $p>0.05$; *: $p<0.05$.

lead to increased antibiotic persistence. Taken together, these results suggest that metabolic dependency on *S. enterica* alone cannot explain antibiotic persistence in *E. coli* in the cross-feeding coculture.

As a supporting piece of evidence to the results in Fig. 3.3, I examined whether metabolic interdependency on the mutualistic partner itself was sufficient to change average expression levels of antibiotic persistence genes in both *E. coli* and *S. enterica*. To achieve this goal, I analyzed the RNA-sequencing data (Table 1) collected by other lab members, Graduate Student Leno Smith Jr. and Postdoctoral Fellow Dr. Jonathan Martinson. Prior to RNA-sequencing, *E. coli* and *S. enterica* were grown to log phase in

a

E. coli	Encoded Proteins Involved in Regulating Persistence	Difference?
relA	(p)ppGpp synthetase	No sig. change
relE	ribosome-dependent or -independent mRNA endonucleases; mRNA interferase toxin	No sig. change
mazF	ribosome-dependent or -independent mRNA endonucleases; endoribonuclease toxin	No sig. change
hipA	Type II toxin: phosphorylated serine/threonine kinase	No sig. change
hipB	Type II antitoxin/DNA-binding transcriptional repressor	No sig. change
spoT	(p)ppGpp synthetase (of the bifunctional synthetase/hydrolase)	No sig. change
dgcI	Putative diguanylate cyclase	↑ Mutualism
krssB	regulator of RpoS	No sig. change
rpoS	RNA polymerase, sigma S (sigma 38) factor	No sig. change
recX	RecA inhibitor	No sig. change
recA	DNA recombination/repair protein	No sig. change
tisB	membrane-depolarizing Type I toxin	No sig. change
istR	small regulatory RNA Type I antitoxin	↑ Mutualism
obgE	GTPase	No sig. change
hokB	Type I toxin	No sig. change
sokB	Putative small regulatory RNA Type I antitoxin	No sig. change
lon	protease: degrades Type II antitoxins in response to (p)ppGpp activity/ oxidative stress	No sig. change
clpS	specificity factor for ClpA-ClpP chaperone-protease complex	No sig. change
clpP	ATP-dependent Clp protease: degrades Type II antitoxins in response to (p)ppGpp activity/oxidative stress	No sig. change
symE	Type I toxin	No sig. change
symR	Small regulatory RNA Type I antitoxin	No sig. change
yafQ	Ribosome-dependent mRNA interferase Type II toxin	No sig. change
mqsA	Type II antitoxin, of the MqsRA toxin-antitoxin system / DNA-binding transcriptional repressor MqsA	No sig. change
mqsR	Type II toxin, mRNA interferase of the MqsR-MqsA toxin-antitoxin system	No sig. change
gltX	Glutamate tRNA ligase	No sig. change
dinJ	Type II antitoxin/DNA-binding transcriptional repressor	No sig. change
yafN	Type II antitoxin	No sig. change
yafO	Type II toxin/ribosome-dependent mRNA interferase	No sig. change
glpD	aerobic glycerol 3-phosphate dehydrogenase	No sig. change

b

S. enterica	Encoded Proteins Involved in Regulating Persistence	Difference
relA	(p)ppGpp synthetase (GTP diphosphokinase)	No sig. change
relE	ribosome-dependent or -independent mRNA endonucleases; mRNA interferase toxin (addiction module toxin)	No sig. change
spoT	(p)ppGpp synthetase (of the bifunctional synthetase/hydrolase)	No sig. change
yjcC, yeaJ, yegE, yaiC, yfiN, yedQ	(Putative) diguanylate cyclase	No sig. change
ylaB	Putative diguanylate cyclase/phosphodiesterase domain 2	No sig. change
doeR	DNA-binding transcriptional repressor	No sig. change
acrR	DNA-binding transcriptional repressor	No sig. change
STM1827	Putative diguanylate cyclase/phosphodiesterase	No sig. change
STM0343	Putative diguanylate cyclase/phosphodiesterase domain 1	No sig. change
PSLT032	Putative diguanylate cyclase/phosphodiesterase	No sig. change
yfeA	Putative diguanylate cyclase/phosphodiesterase domain 1 containing protein	No sig. change
STM1697	Putative diguanylate cyclase/phosphodiesterase domain 2	No sig. change
yhjK	Putative diguanylate cyclase/phosphodiesterase	No sig. change
ygbI	DeoR family transcriptional regulator	No sig. change
rpoS	RNA polymerase, sigma S (sigma 38) factor	No sig. change
recA	DNA recombination/repair protein	No sig. change
lon	Type II antitoxin protease (against (p)ppGpp/oxidative stress)	No sig. change
clpP	ATP-dependent Clp protease	No sig. change
dinJ	Type II antitoxin/DNA-binding transcriptional repressor	No sig. change
yafQ	Ribosome-dependent mRNA interferase Type II toxin	No sig. change
gltX	Glutamate tRNA ligase	No sig. change
glpD	aerobic glycerol 3-phosphate dehydrogenase	↑ Monoculture
ccdB	Toxin addiction system: toxin	No sig. change
ccdA	toxin-addiction system: antidote	No sig. change
STM3033	VapC toxin family PIN domain ribonuclease	No sig. change
STM3034	VapC antitoxin	No sig. change
brnA	Type II toxin-antitoxin system antitoxin	No sig. change
STM0284	Putative shiga-like toxin A subunit	No sig. change
yefM	Orphan antitoxin	No sig. change
relB	Bifunctional antitoxin/transcriptional repressor	No sig. change
ysdB	Type I toxin-antitoxin system toxin	No sig. change
STM1809	GnsA/GnsB family toxin	No sig. change

Table 1. Few Antibiotic Persistence Genes Have Different Expression Levels between Mono- and Co-culture for *E. coli* (a) and *S. enterica* (b). Expression differences were categorized by the Bonferroni-corrected *p*-values. No sig. change: Bonferroni-corrected $p>0.05$, and there is not gene expression difference for a particular gene between mono- and mutualistic co-culture; upper arrows indicate "significant higher expression" with a Bonferroni-correct $p<0.05$.

either monoculture or mutualistic coculture in liquid Hypho medium. The mRNA levels of all ~30 genes related to antibiotic persistence in the review by Harms et al. (2016) were compared between mono- and co-culture. For both species, no significant changes in gene expression were seen in a majority of persistence-related genes (Table 1). For *E. coli* (Table 1a), only two out of 29 genes had an increased expression in the mutualistic coculture (Bonferroni-corrected $p<0.05$). Both genes, *dgcI* (Katharios-Lanwermeyer et al., 2022) and *istR* (Rotem et al., 2010), were associated with regulation of persister formation. On the other hand, only one out of 37 persistence-related genes in *S. enterica* showed an increased expression in monoculture (Table 1b). This gene, *glpD*, was associated with persister formation (Spoering et al., 2006).

Consistent with the fact that only ~5% of known persistence-related genes have

expression differences between monoculture and the cross-feeding coculture (Table 1), I observed little persistence difference in the liquid experiment (Fig. 3.3b). Taken together, these results demonstrate that metabolic interdependency between *E. coli* and *S. enterica* alone cause few differences in the expression level of antibiotic persistence genes between mono- and co-culture, supporting the lack of persistence differences in *E. coli* in the shaken liquid condition.

Results in Section III.1.3 demonstrated that cross-feeding alone could not increase the *E. coli* antibiotic persistence (Fig. 3.3), probably because few persistence-related genes would gain heightened expressions in the cross-feeding condition (Table 1). As a result, Hypothesis 2 is falsified.

III.1.4. Average Growth Rates Cannot Explain Persistence Differences

Following results above, I tested Hypothesis 3 that the antibiotic persistence differences in *E. coli* can be attributed to average growth rate differences. First, I studied the growth rate of *E. coli* populations when grown at 37 ^{o}C on ampicillin-free nitrocellulose membranes in monoculture and in cross-feeding with *S. enterica* (Fig. 3.4a). To measure *E. coli* growth rates, I fit a linear line to the log-transformed CFU measured on nitrocellulose membranes at each harvesting time point. I found that *E. coli* barely grew in either mono- or co-culture over the first 2-hour incubation (One-way ANOVA, p=0.997), and its growth rates barely differed over the entire 4-hour period I tested (One-way ANOVA, p=0.0719). The data show that the difference in antibiotic persistence of *E. coli* between mono- and co-culture can exist without average growth

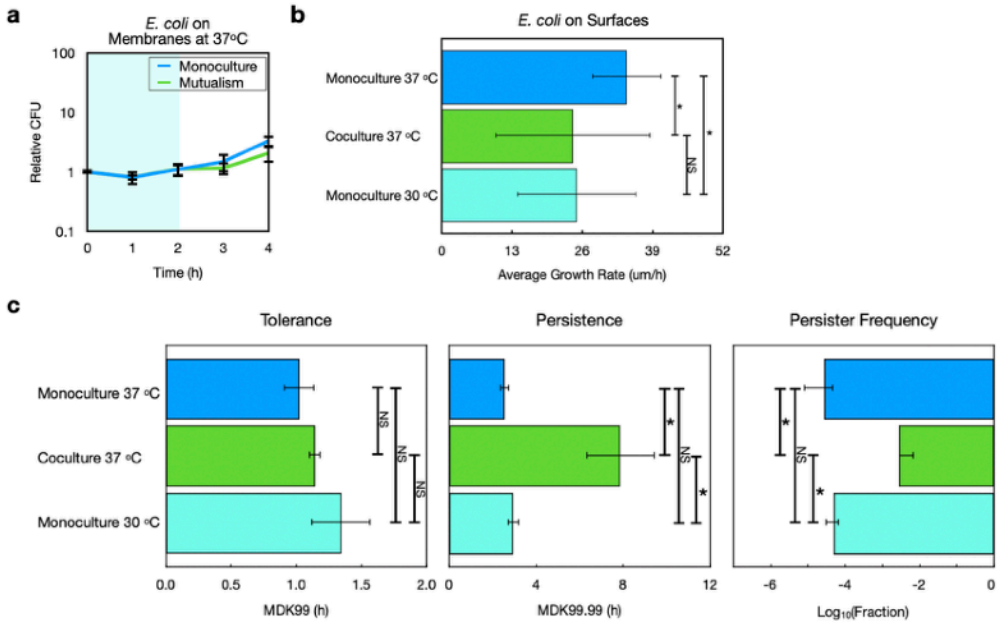

Figure 3.4. Difference in Average *E. coli* Growth Rate Does Not Explain Antibiotic Persistence Differences on Surfaces. **a** At 37 °C, *E. coli* growth on nitrocellulose membranes does not differ drastically within 4 hours of incubation between mono- and co-culture. **b** On agar surfaces, average growth rates of *E. coli* colonies depend on growth temperature and the presence of cross-feeding. **c** Average antibiotic tolerance, persistence, and persister frequency measurements for *E. coli* on membranes. All values shown are average measurements from 3 biologically independent trials. Error bars denote standard deviation of these measurements. NS: no significance, $p>0.05$; *: $p<0.05$.

rate differences prior to antibiotic treatment.

To directly examine whether growth rates can affect *E. coli*'s persistence on nitrocellulose membranes, I performed the antibiotic killing experiment with *E. coli* at different incubation temperatures to change average growth rates. It is important to do this experiment because even if *E. coli* shows a potential for growth during ampicillin treatment over a 24-hour period in the killing experiment, such growth can be easily masked by death and cannot be assessed.

To prepare for this experiment, I first used the time-lapsed imaging setup (Section II.1.5) to measure the log-phase growth rate of *E. coli* colonies when spread on Hypho minimal agar (Fig. 3.4b). At 37 °C, *E. coli* grew much faster in monoculture than in

coculture (One-way ANOVA, Tukey's HSD p<1e-7), consistent with measurements in liquid (Fig. S2, Appendix III). Then, I aimed to find an incubation temperature at which the average *E. coli* growth rate in monoculture mimics that in the 37 ^{o}C coculture. I found that on agar, *E. coli* shared similar average growth rates when grown in the 30 ^{o}C monoculture and in the 37 ^{o}C coculture (One-way ANOVA, Tukey's HSD p=0.301). Here, growth rate measurements of *E. coli* colonies on agar were consistent with those in liquid Hypho medium (Fig. S3, Appendix III), which showed the predictive power of the liquid growth rates to their counterparts on agar surfaces. Together, these results suggest that *E. coli* growth rates on agar can be independently varied by changing the incubation temperature.

Given my above discoveries on *E. coli* average growth rates on agar surfaces, I then performed the ampicillin killing experiment on nitrocellulose membranes at 37 ^{o}C and 30 ^{o}C, respectively (Fig. 3.4c). Specifically, I found that despite the observed growth rate differences in monoculture *E. coli* between 37 ^{o}C and 30 ^{o}C, there were few differences in antibiotic tolerance (One-way ANOVA, Tukey HSD's p=0.1914), in antibiotic persistence (One-way ANOVA, Tukey HSD's p=0.2316), nor in persister frequency (One-way ANOVA, Tukey HSD's p=0.999). Consistent with this discovery, I compared the antibiotic response of *E. coli* in the 30 ^{o}C monoculture and in the 37 ^{o}C coculture—two conditions different in ecology but similar in *E. coli* growth rates. I found that while there was no difference in antibiotic tolerance (One-way ANOVA, Tukey HSD's p=0.5346), I observed that antibiotic persistence (One-way ANOVA, Tukey HSD's

p=7e-7) and the persister frequency (One-way ANOVA, Tukey HSD's *p*=0.00151) were both significantly higher in the 37 ^{o}C coculture. Together, these results conclude that on surfaces, average *E. coli* growth rate differences alone cannot explain its antibiotic persistence.

This analysis above raised an important question of why my conclusion did not fit the well-known fact that higher growth rate in shaken liquid medium was associated with higher beta-lactam lethality (e.g. Tuomanen et al., 1986; Lee et al., 2018). One possible reconciliation is that antibiotic killing responses on surfaces are fundamentally different from those in shaken liquid culture. To investigate this possible difference, I repeated antibiotic killing experiments in liquid medium at 37 ^{o}C and 30 ^{o}C (Fig. S2~S4, Appendix III). Indeed, I found that antibiotic tolerance, persistence, and persister frequency in liquid all well-aligned with growth rates. Together, these efforts confirmed that the antibiotic killing response on surface was functionally different from that in shaken liquid.

In summary, all of the data together in this Section demonstrate that on agar surfaces, the average growth rates of *E. coli* alone cannot explain the increased antibiotic persistence in the cross-feeding coculture at 37 ^{o}C. These results validate that antimicrobial killing responses on surface are fundamentally different from those in shaken liquid medium. Thus, I believe that these results falsified Hypothesis 3.

III.1.5. Single-Colony Growth Physiology Can Explain Persistence Differences

To assess whether Hypothesis 4 holds, I studied the growth physiology of *E. coli* on

surfaces at a single-colony resolution. Hypothesis 4 asserts that the spatial structure of the cross-feeding community leads to the heightened antibiotic persistence compared to the monoculture. To test this Hypothesis, I took advantage of the data from the time-lapsed imaging experiment (Sections II.1.5 & III.1.4), and examined the distribution of growth physiology. Besides the average growth rate measurements (Fig. 3.4b), I observed that on agar, the distribution of *E. coli* growth rates (Fig. 3.5a-b) and durations of lag phase (Fig. 3.5c-d) was higher in co- than in either of the mono-culture conditions. Hence, I quantified such variation by calculating the coefficient of variation (CV) of log-phase *E. coli* growth rates for all colonies, and compared the average growth rate CVs from 3 Hypho agar plates with biological replicates (Fig. 3.5b). I found that the growth rate CV in the 37 °C coculture was at least 2-fold higher than those in the monoculture at 37 °C

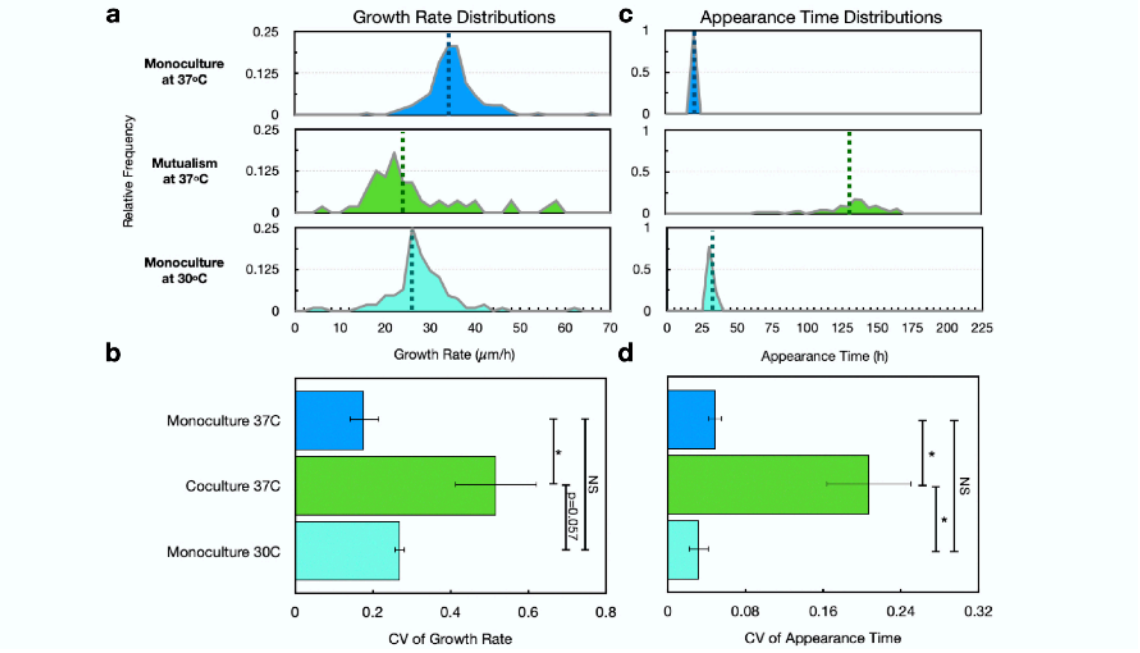

Figure 3.5. Single-Colony Growth Rate and Appearance Time of *E. coli* on Hypho Minimum Agar. **a,c** The distribution of single-colony (**a**) growth rates and (**c**) appearance time of *E. coli* spread on one representative Hypho agar (1) in monoculture at 37 °C, (2) in coculture at 30 °C, and (3) in monoculture at 30 °C. **b,d** Average coefficient of variation (CV) of (**b**) growth rates and (**d**) appearance time from 3 agar plates spread with biologically independent replicates. Error bars denote standard deviation of these measurements. NS: no significance, $p>0.05$; *: $p<0.05$.

(One-way ANOVA, p=0.0227) or at 30 ^{o}C (One-way ANOVA, p=0.0572), respectively. Despite the average growth rate differences between monoculture at 37 ^{o}C and 30 ^{o}C, the growth rate variation did not differ significantly in terms of the CV value (One-way ANOVA, p=0.356).

Also strikingly, I discovered a strong difference in the lag time of *E. coli* when grown in mono- versus co-cultures (Fig. 3.5c-d). One approximate measurement for the duration of *E. coli* lag phase is its appearance time on agar surfaces, which is the time it takes for each individual colonies to grow to be visible for the naked eye (Levin-Reisman et al., 2010). *E. coli* had different average lag times when grown at 37 ^{o}C and 30 ^{o}C in monoculture (Fig. 3.5c, One-way ANOVA, p=3.5e-6). Interestingly, the CV of the lag phase duration did not differ (Fig. 3.5d, One-way ANOVA, p=0.728). In contrast, the lag time CV of *E. coli* in the 37 ^{o}C coculture was much higher than in the 37 ^{o}C monoculture (One-way ANOVA, p=0.000819) and in the 30 ^{o}C monoculture (One-way ANOVA, p=0.000470). When considered together, all data in Fig. 3.5 demonstrated that the heightened antibiotic persistence in coculture grown on surfaces can be explained by the variation but not only the average value of the single-colony growth rate and lag time. Combined with previous research, my data here suggested that the heightened persistence of coculture *E. coli* can be primarily explained by the increased variance in both growth rates and lag time.

Given the large variation in the single-colony growth rate and lag time of *E. coli* grown in the cross-feeding coculture (Fig. 3.5c-d) and their known contribution to

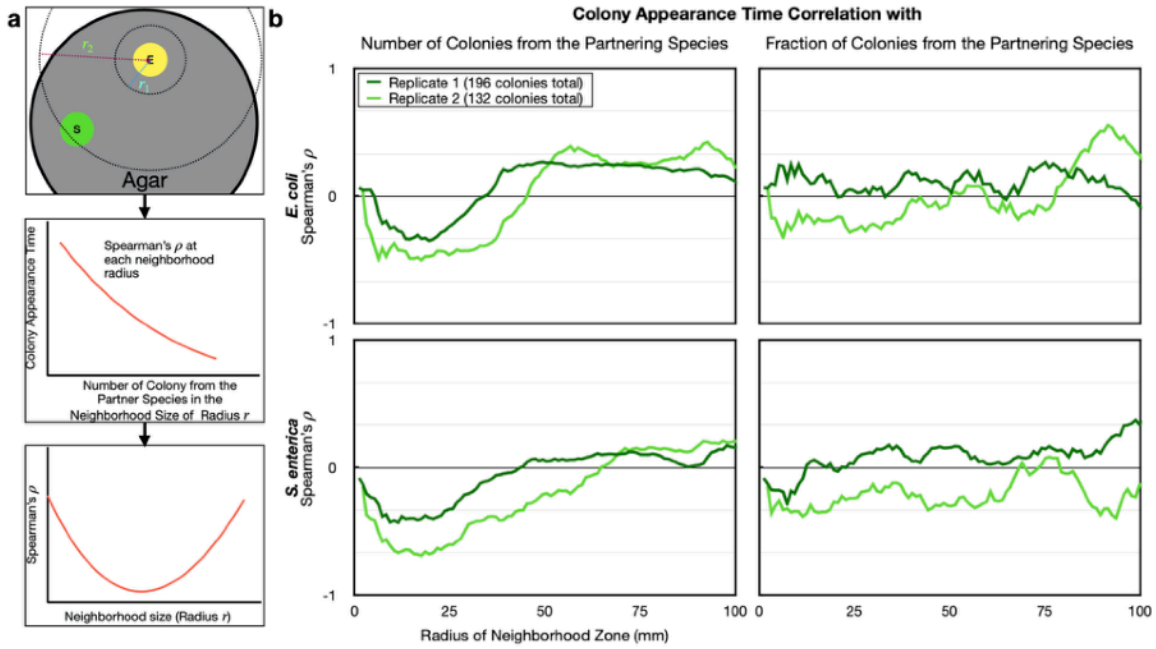

Figure 3.6. Correlation between Colony Appearance Time and Size of the Neighborhood Zone. a The appearance time of individual *E. coli* cells was Spearman-correlated with either (1) the number of *S. enterica* cells or (2) the fraction of *S. enterica* cells within a circular neighborhood of radius, *r*. The estimated correlation parameter, Spearman's ρ, was then plotted against the neighborhood size, *r*. **b** The Spearman's ρ was plotted against the neighborhood size, *r*, for both *E. coli* and *S. enterica*.

antibiotic persistence (Kaplan et al., 2021; Brauner et al., 2016), I sought to study what leads to such variation. One possible reason is that the growth physiology of each individual *E. coli* cell depends on cells in the partnering species within a neighborhood (Dal Co et al., 2020). Here, I hypothesized that the lag time of individual *E. coli* cells will be negatively correlated with the number or the fraction of *S. enterica* cells within a circular neighborhood of radius, *r* (Fig. 3.6a). I fit a Spearman's correlation to the above hypothesized relationships at each radius, *r*, and plotted the Spearman's ρ with *r* (Fig. 3.6b). I found a large variation in ρ along each *r* when lag time was correlated with the number of *S. enterica* colonies within *r*, but not the fraction of *S. enterica* colonies. These finding showed that the number of *S. enterica* within a neighborhood mattered more than the fraction, supporting previous research (Hynes et al., 2018).

Given the importance of the colony number in the cross-feeding species within r to lag time of the focal species on a single-colony level, I assessed its trend of ρ over r. Expectedly (Fig. 3.6a), there was a minimum value of ρ at a relatively small neighborhood ($r \approx 1.8$ cm for *E. coli*; $r \approx 1.2$ cm for *S. enterica*; Fig. 3.6b), This result indicates that the metabolic interdependency of the two species resulted in an interdependency in lag times, which underlie the persistence-by-lag phenotype in *E. coli*. Furthermore, we have $\rho_{\min}$ between -0.34 and -0.51 for *E. coli* and between -0.42 and -0.67 for *S. enterica*, demonstrating a moderate monotonicity between the colony number of the partnering species and the lag time of individual colonies of the focal species. Together, these data delineated that the lag time of individual bacterial colonies relies upon the cross-feeding species within a small neighborhood. Thus, the metabolic interdependency (due to cross-feeding) together with spatial structure allows the growth physiology of *E. coli* to be closely tied to that of *S. enterica* locally, resulting in a persistence-by-lag phenotype. As a result, Hypothesis 4 was supported.

III.2. Mathematically Modeling Bacterial Colony Growth over Space and Time

Finally, I tested whether the experimental data in Section III.1.5 can be recapitulated by my PDE model simulations of *E. coli* growth in both mono- and co-culture. To achieve this goal, I calculated the growth rate and lag time of individual bacterial colonies in my PDE model using the custom-designed code by fitting a log-linear Baranyi function on the growth curve as in Section II.1.3 (Fig. 3.7a). The distributions of *E. coli* growth rate and lag time and were compared between monoculture and coculture

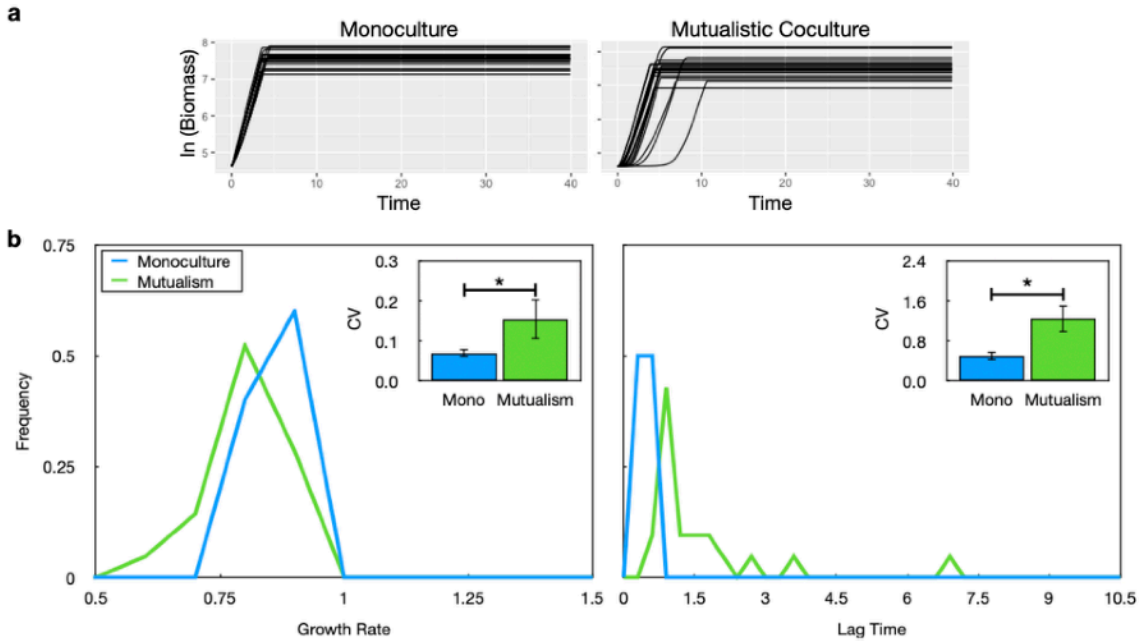

Figure 3.7. Growth of Individual *E. coli* Colonies in PDE Simulations. a Growth curves of *E. coli* colonies that were initially seeded onto a 1-dimension line. The colonies grew by accumulating biomass but did not undergo range expansion. Different growth curves were observed between mono- and the mutualistic co-culture. **b** Each individual colony's growth rate and lag time were calculated by fitting a log-linear Baranyi equation to the growth curves in **a**, and the distribution of these two factors were plotted separately. The CV of 3 independent simulations was calculated and plotted in the inset figures.

(Fig. 3.7b). I found a larger variation in the growth curve trajectories in mutualistic culture than in monoculture (Fig. 3.7a). I further analyzed those variations by looking at the statistical distribution of the growth rate and lag time in 3 simulations with independent initial spatial seeding of *E. coli*. I found that *E. coli* had a higher average growth rate in monoculture than in coculture (One-way ANOVA, $p<0.001$), and the coculture growth rates are more widely distributed than monoculture ones (One-Way ANOVA, $p=0.0471$). Similarly, the average lag time is longer in coculture than in monoculture (One-way ANOVA, $p=0.000796$), and CV is higher in coculture as well (One-way ANOVA, $p=0.0096$), supporting experimental observation of the persistence-by-lag phenotype.

Importantly, the simulation data here demonstrated that even though the maximum *E. coli* growth rate, r_E, was identical in the PDEs for mono- and co-culture, the effective growth rates were different between the two conditions. Furthermore, even though the lag phase of *E. coli* was not taken into account in the PDEs, the elongated lag phase in coculture was an emergent property that appeared in my simulation results. Together, all these data in the mathematical modeling claimed that the combination between metabolic interdependency and spatial structure on agar was sufficient to produce a heightened antibiotic persistence in coculture.

CHAPTER IV: DISCUSSIONS & CONCLUSIONS

IV.1. Thesis Conclusions

In this thesis work, I investigated whether antibiotic persistence was modulated by cross-feeding in a synthetic obligate mutualism of *E. coli* and *S. enterica*. I found that when grown on nitrocellulose membranes on agar, *E. coli* had a ~100-fold higher antibiotic persister frequency in mutualistic coculture with *S. enterica* than in monoculture. However, this heightened antibiotic persistence in *E. coli* was absent when the co-culture was tested in liquid medium or when the mutualism was broken on agar through methionine supplementation. Furthermore, slowing *E. coli* growth rate in monoculture by lowering the temperature did not change antibiotic tolerance or persistence. Together, these results showed that the presence of *S. enterica* alone nor the decreased average growth rate were sufficient to cause the heightened antibiotic persistence on agar.

To further characterize the growth physiology of *E. coli* at a sub-population level, I directly studied the growth rate and lag phase duration of *E. coli* experimentally at a single-colony resolution, and designed a PDE-based mathematical model to simulate *E. coli* growth physiology. Both of these methods demonstrated that cross-feeding on a surface increased the variation in growth rate and lag time, as well as increasing the average lag time. These results suggested that the spatial structure of *E. coli*-*S. enterica* community on the nitrocellulose membrane regulates antibiotic persistence levels in *E. coli* by increasing heterogeneity among cells.

IV.2. Antibiotic Persistence in A Bigger (Spatially-Structured) Picture

IV.2.1. Spatial Structure & Cross-Feeding Increased Phenotypic Heterogeneity

My work has potential implications for antibiotic persistence research, microbial ecology, and clinical microbiology. First, my work demonstrated that the combination of cross-feeding and spatial structure serves as a new mechanism contributing to phenotypic heterogeneity. While many known mechanisms (as reviewed in Section I.2) can contribute to phenotypic heterogeneity, few ecological mechanisms were proposed. Relatively few laboratory studies have investigated the impact of interspecies interactions or spatial structure on heterogeneity in bacterial systems. Clearly, my discoveries here point out the importance of both spatial ecology and interspecies interactions to antibiotic persistence. This result has some similarities to the work by Adamowicz et al. (2018), which showed that cross-feeding can impact AMR; however, in that study, the effect held both in liquid and on agar plates. In comparison, the effect of cross-feeding on antibiotic persistence was only visible in the presence of spatial structure. This differential effect of cross-feeding on agar and in shaken liquid medium supported the significance of cell-to-cell phenotypic heterogeneity in antibiotic persistence, which was heightened by localization of interspecies interactions among cells (Chacón et al., 2018). Together, my work calls for studies to consider the impact of cell-to-cell variability on microbial community function (Holyoak & Wetzel, 2020).

Furthermore, my work laid important groundwork to further investigate the relative contribution of variability in (1) growth rate and (2) lag time to antibiotic persistence.

Focusing first on growth rates, my work found that a high variability in growth rate—but not a significantly lower average value alone—is correlated with the heightened antibiotic persistence in *E. coli* on coculture agar. Interestingly, this finding emphasized the important distinction of antibiotic killing responses of bacteria in the presence or absence of spatial structure. A recent review by Ronneau et al. (2021) argued that antibiotic persistence can be linked to a bimodal distribution of growth rates. In contrast, while I observed a heightened variance in growth rate I did not observe bimodality. This disagreement may exist because analysis of single-cell or single-colony physiology can only deal with a limited number of cells (<200) before the cells occupy the entire microscopic view (Levin-Reisman et al., 2010) or before colonies grow into each other. The persister fraction is definitely smaller than the detection limit (1/200 = 0.5%) in single-cell or single-colony studies, making it difficult to understand the driving force of antibiotic persistence.

On the other hand, my growth rate results agreed with a simpler, threshold-based understanding of antibiotic persistence (Rotem et al., 2010). Both my experimental (Fig. 3.5a) and modeling (Fig. 3.7b) data revealed that with spatial structure, the fraction of cells below a given growth rate threshold was higher in coculture than in monoculture. My work showed that spatial microbial ecology is a unique mechanism contributing to the growth rate heterogeneity in *E. coli*, underlying antibiotic persistence.

My second major discovery was that the combination of spatial structure and cross-feeding caused both high average and high variance in lag time. Results from my PDE

model that only considered nutrient consumption in bacterial growth revealed the increased average and CV in lag time as an emergent property. This result is unique compared to recent research (e.g. Kaplan et al., 2021) that had to incorporate lag times into their mathematical model. My work suggested that the spatial heterogeneity and metabolic dependency (cross-feeding) together made the local growth environment more important than in the shaken liquid condition. Therefore, *E. coli* with longer lag time heterogeneity can appear as an emergent property in the spatially-structured cross-feeding community.

Yet, an unanswered question is whether the heterogeneity in growth rate or lag time effects were the leading cause of antibiotic persistence. A review (Brauner et al., 2016) seems to suggest that persistence-by lag and persistence-by-slow-growth mechanisms are mutually exclusive. My observations of both challenged this perspective. In the Limitations & Future Directions Section (Section IV.3), I propose future experiments to determine the relative contribution of the two mechanisms in isolation and together.

IV.2.2. Mutualism-Stability Relationship: Insights from Microbial Communities

My work also has implications in understanding the highly debated relationship between mutualism and the stability of ecological communities. While much evidence (especially mathematical theories) showed that mutualisms can destabilize ecological communities (May, 1972; May, 2001; Allesina & Tang, 2012; Suweis et al., 2013; Coyte et al., 2015), others provided contrasting evidence by emphasizing the stabilizing effect of mutualism (Mougi & Kondoh, 2012; Rohr et al., 2014; Qian & Akçay, 2020; Stone,

2020; Hale et al., 2020). Settling this debate can close a huge knowledge gap in general ecology, and can also contribute to microbial ecology research. An aspiring goal in microbial ecology is to engineer natural or synthetic microbial communities to "improve human health, agricultural productivity, and climate management"—an effort termed "**microbiome engineering**" (Albright et al., 2022). A better understanding of the role that mutualism plays in community stability can help assess whether mutualisms should be incorporated in microbiome engineering as previously proposed (Kehe et al., 2021).

Here, I argue that the spatially-structured microbial community setup in my research takes advantage of the well-domesticated synthetic microbial mutualism (Harcombe et al., 2014) and so is well-posed to provide further experimental evidence to the debate above. My experimental setup can get around the many limitations in existing studies so far. First, a shared limitation of most studies on this mutualism-community stability relationship is their ignorance on the spatial structure of ecological communities, and the effect of spatial heterogeneity in ecological processes still remains relatively under-studied (Sutherland et al., 2013). Second, most studies reviewed here are theoretical in nature and controlled experiments can be difficult to conduct with macro-ecological communities. In comparison, my experimental setup with microbial communities allows for easy manipulation of species/strain numbers and complexity of interactions (as seen in Hammarlund et al., 2021).

To help settle this aforementioned debate, I can study the stability of *E. coli* populations in the cross-feeding coculture and in monoculture with the ampicillin

perturbation. Stability of an ecological system can be measured by two features of the system: its ecological resistance and ecological resilience (Pimm, 1984). **Ecological resistance** refers to the degree to which the system state (i.e. population size) is changed following a perturbation (i.e. ampicillin), whereas **ecological resilience** measures how fast the system state returns to its equilibrium after the perturbation (Pimm, 1984). In the context of my research, the size of the survived *E. coli* population after ampicillin treatment measured its ecological resistance, while the time it takes for the *E. coli* survivors of ampicillin to grow to the pre-treatment population size would measure its resilience (Angeler et al., 2018).

My results so far allowed me to conclude that spatial structure and cross-feeding together led to higher *ecological* resistance of *E. coli* to the ampicillin perturbation than in monoculture. In essence, spatial structure plays an essential role in this heightened *ecological* resistance due to cross-feeding, which supports the mutualism-stability relationship in the context of microbial communities. Evidently, existing studies assuming spatial homogeneity of ecological communities in their analyses may have overlooked the role of spatial heterogeneity in the mutualism-stability relationship. In particular, my research revealed a mechanism that may be unique to bacterial systems, where the combination of cross-feeding and spatial structure contributes to higher phenotypic diversity in growth physiology. However, whether this mechanism is important in other communities should be further explored. For example, growth physiology of partners in the plant-pollinator mutualism (Hale et al., 2020) may be

drastically different compared to my study, where nutrient diffusion plays a large role in determining growth in the cross-feeding microbial community. Finally, results in my thesis cannot be compared with those in Adamowicz et al. (2018) in the context of ecological resistance. The usage of antibiotics in that study was hardly equivalent to an "ecological perturbation" as the antibiotic was not necessarily at dosages high enough to perturb population size through mechanisms such as killing.

On the other hand, my current research cannot answer whether resilience was affected by the cross-feeding mutualism in the presence of spatial structure. The time it takes for the ampicillin survivors in *E. coli* to grow back to their pre-treatment population densities in mono- and co-culture has not been assessed yet. Despite the higher *E. coli* survival to ampicillin in the cross-feeding coculture than in monoculture, *E. coli* grows more slowly in coculture with *S. enterica* than in monoculture. Thus, whether the higher survival in coculture can compensate for slower growth remains an interesting question to answer. Answers to this question will also contribute to our understanding of the microbial mutualism's stability in antibiotic perturbations. This study of ecological resilience can be further evaluated on an evolutionary time scale (Chomicki et al., 2019), with an evolution experiment including cyclical exposure to ampicillin-high and -free agar (See future directions in Section IV.3). A deeper question to answer there is whether ecological resilience can be maintained over evolutionary cycles.

IV.2.3. Spatial Structure in Polymicrobial Infections in Clinics

Furthermore, my work calls for clinical treatments that take into account spatial

structure of the infection sites. Recent clinical studies in infectious disease began to evaluate interspecies interactions among pathogens (Akala et al., 2021) and between the pathogen and other co-present microbial species (de Vos et al., 2017). However, the complex spatial structure of microbial communities such as biofilms will make it difficult to consider spatial heterogeneity. It has long been known that biofilms in multi-species communities can increase antibiotic tolerance (Burmølle et al., 2006). More alarmingly to the clinical treatment of antibiotics, my work showed that the combination of spatial structure and cross-feeding was sufficient to increase antibiotic persistence in the microbial community. With the high prevalence of positive interactions such as cross-feeding in clinically-relevant bacteria (Flynn et al., 2016; de Vos et al., 2017), the antibiotic persistence levels of these polymicrobial infections may be much higher than previously thought.

Finally, my work implies that cross-feeding may decrease the time needed to evolve for antimicrobial resistance (AMR). Previous *in vitro* (Levin-Reisman et al., 2017) and clinical (Liu et al., 2020) studies with high-concentration, short-termed antibiotic challenges all showed that higher antibiotic tolerance against antimicrobial agents yielded faster evolutionary rate towards antimicrobial resistance, because the higher survival rate gave the bacterial pathogen more opportunities to accumulate AMR mutations. My work clearly found that with spatial structure, there was a higher survival rate of *E. coli* after 5-hour till 24-hour antibiotic treatment in the cross-feeding coculture than in monoculture. This increased antibiotic persistence may likely yield faster AMR evolutions, potentially

causing a bigger problem in treating persistent infections. This intuition clearly contrasts a recent study (Adamowicz et al., 2020) that found a faster evolution rate for AMR in *E. coli* in monoculture than in the cross-feeding coculture when cells were evolved along gradients of antibiotics. However, that study did not include cyclical exposure to high- and low-concentration antibiotics (See Literature Review in Chapter I), and therefore the bacteria were likely to be affected by changes in antibiotic tolerance or persistence.

IV.3. Limitations & Future Directions

One important unanswered question within the scope of my study is what the relative contribution is between the variation in lag time and in growth rate on agar surfaces. Future work will be done to vary either one of the factors and assess antibiotic persistence that way. For example, to only perturb lag phase durations, I can starve *E. coli* alone for a few days (Kaplan et al., 2021) before subjecting them to antibiotic treatment on monoculture agar. My prediction is that while the lag time mean and variation of individual *E. coli* will be significantly affected, their growth rates will not.

Second, a large limitation with my single-colony measurement of growth rate and lag time on agar surfaces is the extremely low density of bacterial cells (Density: ~2.55 cells/cm^2), which is ~10^{-5} of that on my nitrocellulose membrane setups. While this low density does not lead to a problem in monoculture (Levin-Reisman et al., 2010) due to nutrient supplementation in agar, it will amplify the spatial effect for the cross-feeding coculture. Now, I am preparing to set up experiments on agarose pads for time-lapsed microscopy analysis in the near future. With a GFP-labeling plasmid that can assess real-

time metabolism in bacteria (Wang et al., 2017; Deng et al., 2021), I will use the microscopy experiment to acquire measurements on single-cell growth physiology (now for growth rate, lag time, and metabolic rate) at a cell density similar to that in my nitrocellulose membrane setting. Meanwhile, further mathematical modeling is still necessary because it can simplify our understanding of what exactly about spatial structure that led to heightened antibiotic persistence in the cross-feeding coculture. With other parameters been unchanged, I can vary diffusion rates, initial density, or species ratios at the initial time, respectively, in order to evaluate the relative contribution of each factor.

Furthermore, I will consider spatiotemporal evolutionary dynamics (Chomicki et al., 2019) of *E. coli* in the cross-feeding coculture and in monoculture on surfaces. Evolution experiments to evolve for survival against antibiotic perturbations will be completed on agar as in previous liquid experiment (Fridman et al., 2014). In particular, the ampicillin treatment on nitrocellulose membranes will last long enough such that only 10~20 cells survive and form individual colonies. This setup will allow for isolation of each single colony, which can be isolated and grown on new nitrocellulose membranes with the spatial configuration from the previous cycle. In doing so, I will be able to track the spatial and evolutionary dynamics of *E. coli* isolates that are tolerant against antibiotic killing whether interspecies interactions are present or not. The time it takes for the survived colonies to grow back to the cell density pre-treatment can also help me compare the ecological resilience of bacterial systems between co- and mono-culture.

BIBLIOGRAPHY

Ackermann M, et al. (2007). On the evolutionary origin of aging. *Aging Cell* **6**, 235-244.

Ackermann M. (2015). A functional perspective on phenotypic heterogeneity in microorganisms. *Nature Reviews Microbiology* **13**(8), 497-508.

Adamowicz EM, et al. (2018). Cross-feeding modulates antibiotic tolerance in bacterial communities. *ISME Journal* **12,** 2723-2735.

Adamowicz EM, et al. (2020). Cross-feeding modulates the rate and mechanism of antibiotic resistance evolution in a model microbial community of *Escherichia coli* and *Salmonella enterica*. *PLoS Pathogen* **16**(7), e1008700.

Ahmed W, et al. (2015). Distributions of faecal markers in wastewater from different climatic zones for human faecal pollution tracking in Australian surface waters. *Applied Environmental Microbiology* **82**, 1316-1323.

Akala HM, et al. (2021). *Plasmodium* interspecies interactions during a period of increasing prevalence of *Plasmodium ovale* in symptomatic individuals seeking treatment: An observational study. *Lancet* **2**, E141-150.

Albright MBN, et al. (2022). Solutions in microbiome engineering: Prioritizing barriers to organism establishment. *ISME Journal* **16**, 331-338.

Allesina S & Tang S. (2012). Stability criteria for complex ecosystems. *Nature* **483**, 205-208.

Andrews JM. (2001). Determination of minimum inhibitory concentrations. *The Journal of Antimicrobial Chemotherapy* **48**, S5-S16.

Angeler DG, et al. (2018). Resilience in Environmental Risk and Impact Assessment: Concepts and Measurement. *Bulletin of Environmental Contamination and Toxicology* **101,** 543-8.

Antimicrobial Resistance Collaborators. (2022). Global burden of bacterial antimicrobial resistance in 2019: A systematic analysis. *Lancet* **399**, 629-655.

Aranda-Diaz A, et al. (2020). Bacterial interspecies interactions modulate pH-mediated antibiotic tolerance. *Elife* **9**, e51493.

Arani BMS, et al. (2021). Exit time as a measure of ecological resilience. *Science*, **372**(6547), eaay4895.

Armstrong JB & Schindler DE. (2011). Excess digestive capacity in predators reflects a life of feast and famine. *Nature* **476**,84-87.

Baba T, et al. (2006). Construction of *Escherichia coli* K-12 in-frame, single-gene knockout mutants: the Keio collection. *Molecular Systems Biology* **2**(1), 2006.0008.

Bairey E, et al. (2016). High-order species interactions shape ecosystem diversity. *Nature Communications* **7**, 12285.

Balaban NQ, et al. (2004) Bacterial persistence as a phenotypic switch. *Science* **305**,

1622-1625.
Balaban NQ, et al. (2019). Definitions and guidelines for research on antibiotic persistence. *Nature Reviews Microbiology* **17**, 441-448.
Baranyi J & Roberts TA. (1994). A dynamic approach to predicting bacterial growth in food. *International Journal of Food Microbiology* **23**, 277-294.
Bigger JW. (1944). Treatment of staphylococcal infections with penicillin by intermittent sterilization. *Lancet* **244**, 497–500.
Bokinsky G, et al. (2013). HipA-triggered growth arrest and β-lactam tolerance in *Escherichia coli* are mediated by RelA-dependent ppGpp synthesis. *Journal of Bacteriology* **195**(14), 3173-3182.
Bouchaud JP. (1992). Weak ergodicity breaking and aging in disordered-systems. *Journal de Physique I* **2**, 1705–1713.
Brauner A, et al. (2016). Distinguishing between resistance, tolerance and persistence to antibiotic treatment. *Nature Reviews Microbiology* **14,** 320-330.
Brauner A, et al. (2017). An Experimental Framework for Quantifying Bacterial Tolerance. *Biophysics Journal* **112**, 2664-2671.
Bronstein JL. (2015). *Mutualism*. (Oxford University Press, UK).
Burmølle M, et al. (2006). Enhanced biofilm formation and increased resistance to antimicrobial agents and bacterial invasion are caused by synergistic interactions in multispecies biofilms. *Applied & Environmental Microbiology* **72**,3916-3923.
Bush K, et al. (2011). Tackling antibiotic resistance. *Nature Review Microbiology* **9**, 894-896.
Buss da Silva N, et al. (2019). Optimization of turbidity experiments to estimate the probability of growth for individual bacterial cells. *Food Microbiology* **83**, 109-112.
CDC. (2019). *Antibiotic Resistance Threats in the United States*, 2019. Atlanta, GA: U.S. Department of Health and Human Services, CDC.
Chacón JM, et al. (2018). The spatial and metabolic basis of colony size variation. *ISME Journal* **12**, 669-680.
Chomicki G, et al. (2019). The impact of mutualisms on species richness. *Trends in Ecology Evolution* **34**, 698-711.
Connell JL, et al. (2014). Real-time monitoring of quorum sensing in 3D-printed bacterial aggregates using scanning electrochemical microscopy. *Proceedings of the National Academy of Sciences of the United States of America* **111**, 18255-18260.
Coyte KZ, et al. (2015). The ecology of the microbiome: Networks, competition, and stability. *Science* **350**(6261), 663-666.
Cunha BA & Ortega AM. (1995). Antibiotic failure. *The Medical Clinics of North America* **79**(3), 663-672.
Currie CJ, et al. (2014) Antibiotic treatment failure in four common infections in UK

primary care 1991-2012: Longitudinal analysis. *BMJ* **349**, g5493.
Dai L, et al. (2012). Generic indicators for loss of resilience before a tipping point leading to population collapse. *Science* **336**, 1175-1177.
Dal Bello M, et al. (2021). Resource–diversity relationships in bacterial communities reflect the network structure of microbial metabolism. *Nature Ecology & Evolution* **5,** 1424-1434.
Dal Co A, et al. (2019). Emergent microscale gradients give rise to metabolic cross-feeding and antibiotic tolerance in clonal bacterial populations. *Philosophical Transactions of the Royal Society B* **374**, 2019008020190080.
Dal Co A, et al. (2020). Short-range interactions govern the dynamics and functions of microbial communities. *Nature Ecology & Evolution*, **4**(3), 366-375.
Darkoh C, et al. (2015). A rapid and specific method for the detection of indole in complex biological samples. *Applied and Environmental Microbiology* **81**(23), 8093-8097.
Deng Y, et al. (2021). Measuring and modeling energy and power consumption in living microbial cells with a synthetic ATP reporter. *BMC Biology* **19**, 101.
Deter, HS et al. (2021). Antibiotic tolerance is associated with a broad and complex transcriptional response in *E. coli*. *Scientific Reports* **11**, 6112.
Eagle H & Musselman AD. (1948). The rate of bactericidal action of penicillin in vitro as a function of its concentration, and its paradoxically reduced activity at high concentrations against certain organisms. *The Journal of Experimental Medicine* **88**(1), 99–131.
Fleming A. (1945). *Penicillin*. Nobel Prize Lecture, Stockholm, Sweden.
Floss HG & Yu TW. (2005). Rifamycin-mode of action, resistance, and biosynthesis. *Chemical Review* **105**(2), 621-632.
Flynn JM, et al. (2016). Evidence and role for bacterial mucin degradation in cystic fibrosis airway disease. *PLoS Pathogen* **12**, e1005846.
Foster KR & Bell T. (2012). Competition, not cooperation, dominates interactions among culturable microbial species. *Current Biology* **22**, 1845-1850.
Fridman O, et al. (2014). Optimization of lag time underlies antibiotic tolerance in evolved bacterial populations. *Nature* **513**, 418-421.
Fritts RK, et al. (2021). Extracellular metabolism sets the table for microbial cross-feeding. *Microbiology and Molecular Biology Reviews* **85**(1), e00135-20.
Garcia MS. (2009). Early antibiotic treatment failure. *International Journal of Antimicrobial Agents* **34**, S14-S19.
Girgis HS, et al. (2012). Large mutational target size for rapid emergence of bacterial persistence. *Proceedings of the National Academy of Sciences of the United States of America* **109**, 12740–12745.

Ghoul M & Mitri S. (2016). The ecology and evolution of microbial competition. *Trends in Microbiology* **24**, 833-845.

Goldford JE, et al. (2018). Emergent simplicity in microbial community assembly. *Science* **361**(6401), 469-474.

Hale KRS, et al. (2020). Mutualism increases diversity, stability, and function of multiplex networks that integrate pollinators into food webs. *Nature Communications* **11**, 2182.

Hammarlund SP, et al. (2019). A shared limiting resource leads to competitive exclusion in a cross−feeding system. *Environmental Microbiology* **21**, 759-771.

Hammarlund SP, et al. (2021). Limitation by a shared mutualist promotes coexistence of multiple competing partners. *Nature Communications* **12**, 1-8.

Harcombe WR. (2010). Novel cooperation experimentally evolved between species. *Evolution* **64**, 2166-2172.

Harcombe WR, et al. (2014). Metabolic resource allocation in individual microbes determines ecosystem interactions and spatial dynamics. *Cell Reports* **7**, 1104-1115.

Harcombe WR, et al. (2018). Evolution of bidirectional costly mutualism from byproduct consumption. *Proceedings of the National Academy of Sciences of the United States of America* **115**, 12000-12004.

Harms A, et al. (2016). Mechanisms of bacterial persistence during stress and antibiotic exposure. *Science* **354**, aaf4268.

Hauryliuk V, et al. (2015). Recent functional insights into the role of (p) ppGpp in bacterial physiology. *Nature Reviews Microbiology* **13**, 298-309.

Hobby GL, et al. (1942). Observations on the Mechanism of Action of Penicillin. *Proceedings of the Society for Experimental Biology and Medicine* **50**(2), 281-285.

Hoek TA, et al. (2016). Resource Availability Modulates the Cooperative and Competitive Nature of a Microbial Cross-Feeding Mutualism. *PLoS Biology* **14**(8), e1002540.

Holyoak M & Wetzel W. (2020). Variance-Explicit Ecology: A Call for Holistic Study of the Consequences of Variability at Multiple Scales. *In* Dobson A, Tilman D & Holt R (Ed), *Unsolved Problems in Ecology* (pp. 25-42). Princeton: Princeton University Press.

Human Microbiome Project Consortium. (2012). Structure, function and diversity of the healthy human microbiome. *Nature* **486**, 207-214.

Hynes WF, et al. (2018). Bioprinting microbial communities to examine interspecies interactions in time and space. *Biomedical Physics & Engineering Express* **4**, 055010.

Jaurin B & Normark S. (1983). Insertion of IS2 creates a novel *ampC* promoter in

Escherichia coli. Cell **32**, 809-816.
Johnson PJT & Levin BR. (2013). Pharmacodynamics, Population Dynamics, and the Evolution of Persistence in *Staphylococcus aureus*. *PLoS Genetics* **9**(1), e1003123.
Kaplan Y, et al. (2021). Observation of universal ageing dynamics in antibiotic persistence. *Nature* **600**, 290-294.
Katharios-Lanwermeyer S, et al. (2022). The Diguanylate Cyclase YfiN of Pseudomonas aeruginosa Regulates Biofilm Maintenance in Response to Peroxide. *Journal of Bacteriology* **204**(1), e0039621.
Kærn M, et al. (2005). Stochasticity in gene expression: from theories to phenotypes. *Nature Reviews Genetics* **6,** 451-464.
Kehe J, et al. (2021). Positive interactions are common among culturable bacteria. *Science Advances* **7**(45), eabi7159.
Kiviet D, et al. (2014). Stochasticity of metabolism and growth at the single-cell level. *Nature* **514,** 376-379.
Korch SB, et al. (2003). Characterization of the *hipA7* allele of *Escherichia coli* and evidence that high persistence is governed by (p)ppGpp synthesis. *Molecular Microbiology* **50**(4), 1199-1213.
Kuroda A, et al. (1997). Guanosine tetra- and penta-phosphate promote accumulation of inorganic polyphosphate in *Escherichia coli*. *Journal of Biological Chemistry* **272**, 21240-21243.
Kuroda A, et al. (2001). Role of inorganic polyphosphate in promoting ribosomal protein degradation by the Lon protease in *E. coli*. *Science* **293**, 705-708.
Lawson CE, et al. (2019). Common principles and best practices for engineering microbiomes. *Nature Reviews Microbiology* **17**, 725-741.
Lee AJ, et al. (2018). Robust, linear correlations between growth rates and β-lactam–mediated lysis rates. *Proceedings of the National Academy of Sciences of the United States of America* **115**, 4069-4074.
Lee S & Lee DK. (2018). What is the proper way to apply the multiple comparison test? *Korean Journal of Anesthesiology* **71**(5), 353-360.
Leszczynska D, et al. (2013). The formation of persister cells in stationary-phase cultures of *Escherichia coli* is associated with the aggregation of endogenous proteins. *PLoS One* **8**, e54737.
Levin BR, et al. (2014). Persistence: a copacetic and parsimonious hypothesis for the existence of non-inherited resistance to antibiotics. *Current Opinion in Microbiology* **21**, 18-21.
Levine JM, et al. (2017). Beyond pairwise mechanisms of species coexistence in complex communities. *Nature* **546**(7656):56-64.
Levin-Reisman I, et al. (2010). Automated imaging with ScanLag reveals previously

undetectable bacterial growth phenotypes. *Nature Methods* **7**(9), 737-739.
Levin-Reisman I, et al. (2017). Antibiotic tolerance facilitates the evolution of resistance. *Science* **355**(6327), 826-830.
Lewis K. (2005) Persister cells and the riddle of biofilm survival. *Biochemistry (Moscow)* **70**, 267-274.
Lewis K. (2010). Persister cells. *Annual Review Microbiology* **64**, 357-372.
Liu Q et al. (2013). Phase separation explains a new class of self-organized spatial patterns in ecological systems. *Proceedings of the National Academy of Sciences of the United States of America* **110**(29), 11905-11910.
Liu J, et al. (2020). Effect of tolerance on the evolution of antibiotic resistance under drug combinations. *Science* **367**, 200-204.
Lopatkin AJ, et al. (2019), Bacterial metabolic state more accurately predicts antibiotic lethality than growth rate. *Nature Microbiology* **4**, 2109-2117.
May RM. (1972). Will a large complex system be stable? *Nature* **238**, 413-414.
May RM. (2001). *Stability and Complexity in Model Ecosystems.* (Princeton University Press, Princeton, NJ).
Mougi A & Kondoh M. (2012). Diversity of interaction types and ecological community stability. *Science* **337**, 349-351.
Moyed HS & Bertrand KP. (1983). HipA, a newly recognized gene of *Escherichia coli* K-12 that affects frequency of persistence after inhibition of murein synthesis. *Journal of Bacteriology* **155**, 768.
Munita JM & Arias CA. (2016). Mechanisms of Antibiotic Resistance. *Microbiology Spectrum* **4**, 10.
Orman MA, et al. (2013). Dormancy is not necessary or sufficient for bacterial persistence. *Antimicrobial Agents & Chemotherapy* **57**, 3230-3239.
Pimm SL. (1984). The complexity and stability of ecosystems. *Nature* **307,** 321-326.
Poirel L, et al. (2005). Origin of plasmid-mediated quinolone resistance determinant QnrA. *Antimicrobial Agents & Chemotherapy* **49**, 3523-3525.
Potrykus K & Cashel M. (2008). (p)ppGpp: still magical? *Annual Review in Microbiology* **62**, 35-51.
Qian JJ & Akçay E. (2020). The balance of interaction types determines the assembly and stability of ecological communities. *Nature Ecology & Evolution* **4,** 356-365.
Ratzke C, et al. (2020). Strength of species interactions determines biodiversity and stability in microbial communities. *Nature Ecology & Evolution* **4**, 376-383.
Reardon, S. (2014). WHO warns against 'post-antibiotic' era. Nature.
Reygaert WC. (2018). An overview of the antimicrobial resistance mechanisms of bacteria. *AIMS Microbiology* **4**(3), 482-501.
Rittenbury MS. (1990). How and why aztreonam works. *Surgery, Gynecology &*

Obstetrics **171**, S19-S23.
Rohr RP, et al. (2014). On the structural stability of mutualistic systems. *Science* **345**(6195), 1253497.
Ronneau S, et al. (2021). Antibiotic persistence and tolerance: Not just one and the same. *Current Opinion in Microbiology* **64**, 76-81.
Rotem E, et al. (2010). Regulation of phenotypic variability by a threshold- based mechanism underlies bacterial persistence. *Proceedings of the National Academy of Sciences of the United States of America* **107**, 12541-12546.
R Core Team. (2016). *R: A language and environment for statistical computing.* R Foundation for Statistical Computing, Vienna, Austria.
Sampaio NMV, et al. (2022). Dynamic gene expression and growth underlie cell-to-cell heterogeneity in *Escherichia coli* stress response. *Proceedings of the National Academy of Sciences of the United States of America* **119**(14), e2115032119.
Shaffer ML. (1981). Minimum population sizes for species conservation. *Bioscience* **31**, 131-134.
Stone L. (2020). The stability of mutualism. *Nature Communications* **11,** 2648.
Song S & Wood TK. (2020). A Primary Physiological Role of Toxin/Antitoxin Systems Is Phage Inhibition. *Frontiers in Microbiology* **11**, 1895.
Spoering AL, et al. (2006). GlpD and PlsB participate in persister cell formation in *Escherichia coli*. *Journal of Bacteriology* **188**(14), 5136-5144.
Sutherland WJ, et al. (2013). Identification of 100 fundamental ecological questions. *Journal of Ecology* **101**, 58-67.
Suweis S, et al. (2013). Emergence of structural and dynamical properties of ecological mutualistic networks. *Nature* **500**(7463), 449-452.
Tamer YT, et al. (2021). The Antibiotic Efflux Protein TolC Is a Highly Evolvable Target under Colicin E1 or TLS Phage Selection. *Molecular Biology and Evolution* **38**, 4493-4504.
Tarnita C, et al. (2017). A theoretical foundation for multi-scale regular vegetation patterns. *Nature* **541,** 398-401.
Thiede JM. (2019). *Targeting Mycobacterium tuberculosis intrinsic resistance mechanisms to potentiate antitubercular drug action* (Doctoral Dissertation, University of Minnesota, Minneapolis, MN).
Tillotson G, et al. (2020). Antibiotic Treatment Failure and Associated Outcomes Among Adult Patients With Community-Acquired Pneumonia in the Outpatient Setting: A Real-world US Insurance Claims Database Study, *Open Forum Infectious Diseases* **7**, ofaa065.
Tuomanen E, et al. (1986). The rate of killing of *Escherichia coli* by β-lactam antibiotics is strictly proportional to the rate of bacterial growth. *Journal of General*

Microbiology **132**, 1297-1304.
Turing A. (1952). The Chemical Basis of Morphogenesis. *Philosophical Transactions of the Royal Society of London B* **237**(641), 37-72.
Van den Bergh B, et al. (2016). Frequency of antibiotic application drives rapid evolutionary adaptation of *Escherichia coli* persistence. *Nature Microbiology* **1**, 16020.
Vazquez-Laslop N, et al. (2006) Increased persistence in *Escherichia coli* caused by controlled expression of toxins or other unrelated proteins. *Journal of Bacteriology* **188**, 3494-3497.
Vega NM, et al. (2013). *Salmonella typhimurium* intercepts *Escherichia coli* signaling to enhance antibiotic tolerance. *Proceedings of the National Academy of Sciences of the United States of America* **110**, 14420-14425.
Vulin C, et al. (2018). Prolonged bacterial lag time results in small colony variants that represent a sub-population of persisters. *Nature Communications* **9**, 4074.
Wang T, et al. (2017). Bacterial persistence induced by salicylate via reactive oxygen species. *Scientific Reports* **7**, 43839.
Walsh C & Wencewicz TA. (2016). *Antibiotics: Challenges, Mechanisms, Opportunities*. (ASM Press, Washington DC).
Weller DM, et al. (2002). Microbial populations responsible for specific soil suppressiveness to plant pathogens. *Annual Reviews in Phytopathology* **40**, 309-348 (2002).
Windels EM, et al. (2020). Bacteria under antibiotic attack: Different strategies for evolutionary adaptation. *PLoS Pathogen* **16**(5), e1008431.
World Health Organization. (2014). Antimicrobial resistance: Global report on surveillance. World Health Organization.
Yu JSL, et al. (2022). Microbial communities form rich extracellular metabolomes that foster metabolic interactions and promote drug tolerance. *Nature Microbiology* **7,** 542-555.
Yurtsev EA, et al. (2016). Oscillatory dynamics in a bacterial cross-protection mutualism. *Proceedings of the National Academy of Sciences of the United States of America* **113**(22), 6236-6241.
Zengler K & Zaramela LS. (2018). The social network of microorganisms - How auxotrophies shape complex communities. *Nature Reviews Microbiology* **16**, 383-390.
Zimmer-Faust AG, et al. (2021). A combined digital PCR and next generation DNA-sequencing based approach for tracking nearshore pollutant dynamics along the southwest United States/Mexico border. *Frontiers in Microbiology*, **12**, 674214.

APPENDIX

Appendix I. Supplementary Literature Review

Genetic Mechanisms: Mechanisms on how AMR is gained		
Type	**Definition/Explanation**	**Example**
Intrinsic resistance	Resistance is present due to some innate trait of the bacteria independent of drug selective pressures and is not a result of horizontal gene transfer (Thiede, 2019).	All Gram-positive bacteria are resistant to aztreonam, which only binds well with the protein-binding protein 3 (PBP3) of Gram-*negative* bacteria (Rittenbury, 1990).
Mutational resistance	Resistance is gained when cells are exposed to antibiotics and a subset of bacteria gain mutations that affect the antibiotic activity. Cells with resistant mutations against antibiotics can grow in antibiotics and dominate the population.	*E. coli* evolved in sub-MIC concentrations of ampicillin gain mutations that raise its MIC (Adamowicz et al., 2020).
Horizontal gene transfer-based resistance	Resistance is gained when a cell gets in contact with other cells that carry resistant mutations, and acquire that mutations through horizon gene transfer, a mechanism that allows for DNA to be transferred between bacteria.	Quinolone-resistance in pathogenic *Enterobacteriaceae* is attributed to *qnrA* genes, which were found to be original to the marine/freshwater species, *Shewanella algae* (Poirel et al., 2005).
Biochemical Mechanisms: Mechanisms on how the AMR genes result in the resistant phenotype		
Type	**Definition/Explanation**	**Example**
Modification of the antibiotic molecule	Cells deactivate the antibiotics by changing the chemical structure of the antibiotics by, say, producing antibiotic-cleaving enzymes.	Beta-lactamases are known to cleave the beta-lactam ring in the beta-lactam antibiotics (e.g. penicillin).
Blocking antibiotics from reaching targets	Cells prevent antibiotics from interacting with their targets to limit their activity.	Increased efflux pump TolC expression in *E. coli* can pump piperacillin out of the cell (Tamer et al., 2021).
Modification/ bypass of antibiotic target	Cells modify the target of the antibiotics to lower effective drug-target binding or make drug-target binding unable to disturb the normal cellular activity.	Mutations in the *rpoB* gene—the gene that encodes the beta subunit of the RNA polymerase (RNAP)—can lower affinity of rifampin for the RNAP but maintain RNAP's catalytic activity (Floss & Yu, 2005).

Table S1. Summary of the Genetic and Biochemical Mechanisms of Antibiotic Resistance.

Appendix II. Supplementary Mathematical Analysis

AII.1. Nondimensionalization of the PDE Model

First, I non-dimensionalize the PDE systems in Eqs. [1~2] by defining $y = \frac{x}{Q}$,

$\tau = t_0 t$, $u = \frac{E}{W}$, $s = \frac{S}{W}$, $m = \frac{M}{W}$, $a = \frac{A}{W}$, $l = \frac{L}{W}$, $\delta_m^2 = \frac{D_M}{t_0 Q^2}$, $\delta_a^2 = \frac{D_A}{t_0 Q^2}$, $\delta_l^2 = \frac{D_L}{t_0 Q^2}$,

and $k_i = \frac{K_i}{W}$ for $i \in \{M, L, A\}$. Here, I let $t_0 = t^{-1}$, $Q = 1$ unit of distance, and $W = 1$ cell unit per mL (as in Hammarlund et al., 2021). Therefore, the non-dimensionalized, cross-feeding system in Eq. [1], becomes:

$$\frac{\partial u}{\partial \tau} = \frac{r_E}{t_0}\left(\frac{m}{m + k_M}\right)\left(\frac{l}{l + k_L}\right)u - \frac{\kappa_E}{t_0}u, \quad \text{[A1a]}$$

$$\frac{\partial s}{\partial \tau} = \frac{r_S}{t_0}\left(\frac{a}{a + k_A}\right)s - \frac{\kappa_S}{t_0}s, \quad \text{[A1b]}$$

$$\frac{\partial m}{\partial \tau} = \delta_m^2 \nabla^2 m + \frac{p_M r_S}{t_0}\left(\frac{a}{a + k_A}\right)s - \frac{c_E}{t_0}\left(\frac{m}{m + k_M}\right)\left(\frac{l}{l + k_L}\right)u - \frac{\kappa_M}{t_0}m, \quad \text{[A1c]}$$

$$\frac{\partial a}{\partial \tau} = \delta_a^2 \nabla^2 a + \frac{p_A r_E}{t_0}\left(\frac{m}{m + k_m}\right)\left(\frac{l}{l + k_l}\right)u - \frac{c_S}{t_0}\left(\frac{a}{a + k_a}\right)s - \frac{\kappa_A}{t_0}a, \quad \text{[A1d]}$$

$$\frac{\partial l}{\partial \tau} = \delta_l^2 \nabla^2 l - \frac{c_L}{t_0}\left(\frac{m}{m + k_M}\right)\left(\frac{l}{l + k_L}\right)u - \frac{\kappa_L}{t_0}l. \quad \text{[A1e]}$$

The boundary conditions become:

$$\frac{\partial n}{\partial y} = 0 \text{ at } x = 0,\ 5, \text{ for } n \in \{u, s, m, a, l\}. \quad \text{[A1f]}$$

Similarly, the non-dimensionalized monoculture system of *E. coli* in Eq. [2]

becomes:

$$\frac{\partial m}{\partial \tau} = \delta_m^2 \nabla^2 m - \frac{c_E}{t_0}\left(\frac{m}{m+k_M}\right)\left(\frac{l}{l+k_L}\right)u - \frac{\kappa_M}{t_0}m, \quad \text{[A2a]}$$

$$\frac{\partial u}{\partial \tau} = \frac{r_E}{t_0}\left(\frac{m}{m+k_M}\right)\left(\frac{l}{l+k_L}\right)u - \frac{\kappa_E}{t_0}u, \quad \text{[A2b]}$$

$$\frac{\partial l}{\partial \tau} = \delta_l^2 \nabla^2 l - \frac{c_L}{t_0}\left(\frac{m}{m+k_M}\right)\left(\frac{l}{l+k_L}\right)u - \frac{\kappa_L}{t_0}l, \quad \text{[A2c]}$$

with similar boundary conditions:

$$\frac{\partial n}{\partial y} = 0 \text{ at } x = 0,\ 5, \text{ for } n \in \{u, m, l\}. \quad \text{[A2d]}$$

AII.2. A Lack of Turing Pattern in the Two Population PDE Models

One question of mathematical interest is whether ecological systems can self-organize to form spatial patterns (Liu et al., 2013). One self-organized spatial pattern is the Turing pattern (Turing, 1952), which is a pattern of stripes and spots that arise naturally and autonomously from a homogeneous, uniform state. Example systems showing Turing patterns include mussel populations (Liu et al., 2013) and the combination of sand termites and perennial grasses in southwestern Africa (Tarnita et al., 2017). Here, I study whether the cross-feeding system in our *E. coli*-*S. enterica* community can demonstrate Turing patterns in the concentration of the cross-fed nutrients.

***Proposition 1*:** The system in Eq. [A1] does not produce Turing patterns regarding local densities of the cross-fed nutrient, a and m.

***Proof*:** First, I aim to find a steady state for the spatially uniform system by setting

$\delta_m^2 = \delta_a^2 = \delta_l^2 = 0$. At a steady state, I can write Eq. [A1a] as:

$$\left(\frac{r_E}{t_0} f\left(m, l\right) - \frac{\kappa_E}{t_0}\right) u = 0, \qquad \text{[A3a]}$$

where

$$f\left(m, l\right) = \left(\frac{m}{m + k_M}\right)\left(\frac{l}{l + k_L}\right). \qquad \text{[A3b]}$$

Because the steady state only makes biological sense if it is non-trivial, I must not have $u^S = s^S = 0$ with X^S denoting the steady state solution of variable X. This means that $\left(\frac{r_E}{t_0} f\left(m, l\right) - \frac{\kappa_E}{t_0}\right)^S = \left(\frac{r_S}{t_0} g\left(a\right) - \frac{\kappa_S}{t_0}\right)^S = 0$ must hold with

$$g\left(a\right) = \frac{a}{a + k_A}. \qquad \text{[A3c]}$$

Therefore, I must have $a^S = 0$. Given that we are interested in lactose being present in the environment, I let $l^s > 0$. This means that $a^S = m^S = 0$. It is clear that these two terms do not interact with each other at all at steady states, so no Turing patterns can exist for these two variables. ■

AII.3. Parametrization of the PDE Model

Variables in Eqs. [1~2] take values in Table S2. At the initial time point ($t = 0$), twenty locations were selected randomly on the 1D line to seed biomass of *E. coli* (and *S. enterica*, if in the mutualism model). In the mutualism model, the initial biomass was set to be $E\left(t = 0, x_i\right) = 100$ and $S\left(t = 0, x_j\right) = 100$ for *E. coli* and *S. enterica*,

respectively, at locations x_i or x_j. On the entire 1D line, initial lactose was set to be $L\,(t = 0,x) = 1000\,\forall x$, methionine and acetate was seeded at $M\,(t = 0,x) = 0.01$ and $A\,(t = 0,x) = 0.01$ for all x. Similarly in the monoculture model, I had $E\left(t = 0,x_i\right) = 100$ as initial *E. coli* biomass in 20 randomly selected locations. No acetate or *S. enterica* was present in the model. The initial lactose and methionine concentrations were $L\,(t = 0,x) = M\,(t = 0,x) = 1000$ for all x.

Parameter	Unit	Value	Biological Interpretation	Source
x	Arbitrary unit of distance	1	Unit of space.	Definition
t	Arbitrary unit of time	1	Unit of time.	Definition
Y	Arbitrary unit of distance	5	Total size of the 1-dimension modeling canvas.	Definition
E, S, M, A, L	Cell unit/mL	-	*E. coli*, *S. enterica*, methionine, acetate, and lactose, respectively.	Definition; Hammarlund et al. (2021)
D_M	x^2/t	0.01	Diffusion constant of methionine.	Estimated based on Chacón et al. (2018)
D_A, D_L	x^2/t	0.05	Diffusion constants of the acetate and lactose sugars.	Estimated based on Chacón et al. (2018)
p_M	Unitless	1.56	Production rate of methionine by *S. enterica*.	Hammarlund et al. (2021); adjusted with unpublished laboratory data
p_A	Unitless	1.01	Production rate of acetate by *E. coli*.	Hammarlund et al. (2021); adjusted with unpublished laboratory data
c_E	t^{-1}	0.1	*E. coli* consumption rate of methionine.	Hammarlund et al. (2021); adjusted with unpublished laboratory data
c_L	t^{-1}	1.0	*E. coli* consumption rate of lactose.	Hammarlund et al. (2021); adjusted with unpublished laboratory data
c_S	t^{-1}	1	*S. enterica* consumption rate of acetate.	Hammarlund et al. (2021); adjusted with unpublished laboratory data
r_E	t^{-1}	1	*E. coli* maximum growth rate.	Hammarlund et al. (2021)
r_S	t^{-1}	0.5	*S. enterica* maximum growth rate.	Hammarlund et al. (2021)
K_M, K_A, K_L	Cell unit/mL	1	Half-saturation methionine, acetate, lactose concentration for bacterial growth.	Hammarlund et al. (2021); adjusted for simplicity
κ_E, κ_S, κ_M, κ_A, κ_L	t^{-1}	5E-09	Natural decay rate of *E. coli*, *S. enterica*, methionine, acetate, and lactose.	Estimated and adjusted for simplicity

Table S2. Parameters Used in the PDE Model.

Appendix III. Supplementary Result Figures

AIII.1. Indole Production on Nitrocellulose Membranes

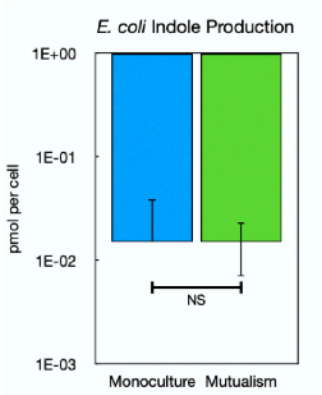

Figure S1. *E. coli*'s Indole Production Does not Differ between Monoculture and Mutualistic Coculture on Surfaces. Indole concentration per *E. coli* cell was measured on the nitrocellulose membrane setup as in Section II.1.4 for all *E. coli*. *E. coli* CFU was then used to calculate indole production per cell. The production of indole over 2 hour ampicillin-free incubation was not different between mono- and co-culture with *S. enterica* (One-way ANOVA, p=0.9918). Error bars denote standard deviation of 3 biologically independent trials. NS: no significance, p>0.05.

AIII.2. Antibiotic Killing Response in Liquid and on Surfaces

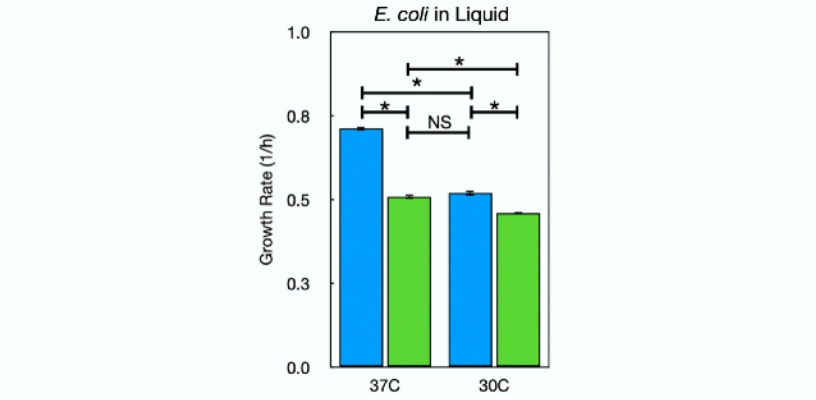

Figure S2. *E. coli* Growth Rate in Shaken Liquid Hypho Medium. Grow rate of *E. coli* was measured in log-phase in liquid Hypho minimum medium by tracking the constitutively-expressed CFP signal level over time. The *E. coli* growth rate is affected by cross-feeding (Two-way ANOVA, F[1]=1071.1, p=8.29e-10), temperature (Two-way ANOVA, F[1]= 923.6, p=1.49e-9), and the interaction between the two factors (Two-way ANOVA, F[1]= 303.1, p=1.21e-7). Specifically, *E. coli* grows much faster in monoculture than in the cross-feeding coculture when the growth temperature is the same (Two-way ANOVA; Tukey's HSD p<1e-8 for 37 ^{o}C; Tukey's HSD p=0.0000218 for 30 ^{o}C). Also, *E. coli* expectedly grows faster at higher temperatures in the same ecological condition (Two-way ANOVA; Tukey's HSD p<1e-8 for monoculture; Tukey's HSD p=7.44e-5 for the cross-feeding coculture). Interestingly, the *E. coli* growth rate in the cross-feeding coculture at 37 ^{o}C is not significantly different from its counterpart in monoculture at 30 ^{o}C (Two-way ANOVA, Tukey's HSD p=0.4050). This growth rate trend matches that on agar (Fig. 3.4b). Error bars denote standard deviation of 3 biologically independent trials. NS: no significance, p>0.05.

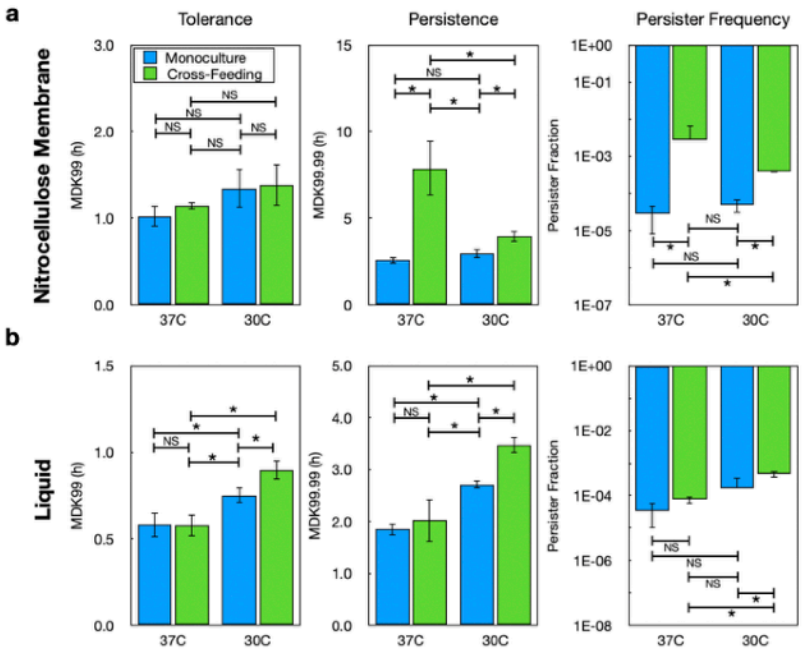

Figure S3. *E. coli* Response to Ampicillin Killing on Surfaces (a) and in Shaken Liquid (b). a Antibiotic tolerance of *E. coli* is associated with temperature (Two-way ANOVA, p=0.0238) alone, but not cross-feeding alone (Two-way ANOVA, p=0.4430) nor the interaction between them (Two-way ANOVA, p=0.7071). Persistence in *E. coli* showed a different trend. Persistence was associated with temperature (Two-way ANOVA, p=0.00545) and cross-feeding (Two-way ANOVA, p=0.000154) separately, and the interaction between them (Two-way ANOVA, p=0.00177). However, the antibiotic persistence measurement, $MDK_{99.99}$, depends on antibiotic tolerance, MDK_{99}. Thus, the statistically significant correlations here only suggest an inheritance of the effects on antibiotic tolerance. Persister frequency was barely correlated with temperature alone (Two-way ANOVA, p=0.0951), cross-feeding alone (Two-way ANOVA, p=0.0744), or the interaction between them (Two-way ANOVA, p=0.0948). **b** In liquid, temperature (Two-way ANOVA, p=8.82e-5) and cross-feeding (Two-way ANOVA, p=0.0458) separately had a significant impact on antibiotic tolerance, but not the interaction between the two factors (Two-way ANOVA, p=0.0561). Persistence in liquid could be explained by temperature (Two-way ANOVA, p=2.26e-5) and cross-feeding alone (Two-way ANOVA, p=0.00757), but barely by the interaction between them (Two-way ANOVA, p=0.0579). And the persister frequency could be explained by temperature (Two-way ANOVA, p=8.12e-05) and cross-feeding alone (Two-way ANOVA, p=0.00156), and by the interaction between them (Two-way ANOVA, p=0.00753). Error bars denote standard deviation of 3 biologically independent trials. NS: no significance, p>0.05. *: statistically significant, p<0.05.

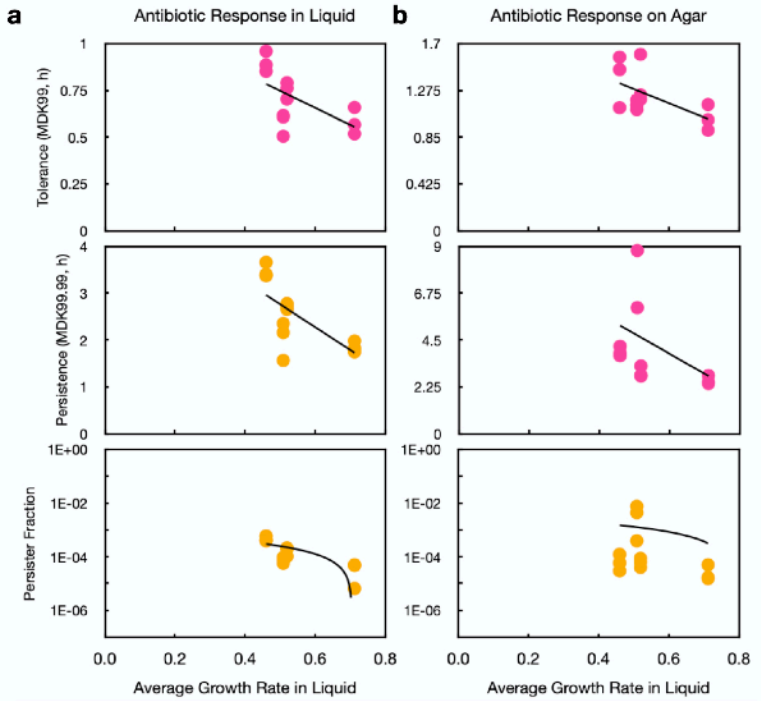

Figure S4. Correlation between Growth Rate of *E. coli* in Liquid Hypho Medium and Its Antibiotic Response in (a) Liquid and (b) on Nitrocellulose Membranes. Each dot was a single data point. A linear line was fitted between growth rate and antibiotic tolerance, persistence, and persister fraction. Note that the linear fit on the persister fraction data looked curvy because the *y*-axis was log-transformed. **a** In liquid, there was a significant correlation for tolerance (Adjusted R^2=0.317, p=0.0331), persistence (Adjusted R^2=0.4425, p=0.0109), and persister frequency (Adjusted R^2=0.381, p=0.0193). **b** On surfaces, there was only a significant correlation for tolerance (Adjusted R^2=0.2971, p=0.0388), but not for persistence (Adjusted R^2=0.09125, p=0.178) or persister frequency (Adjusted R^2=-0.0436, p=0.515).

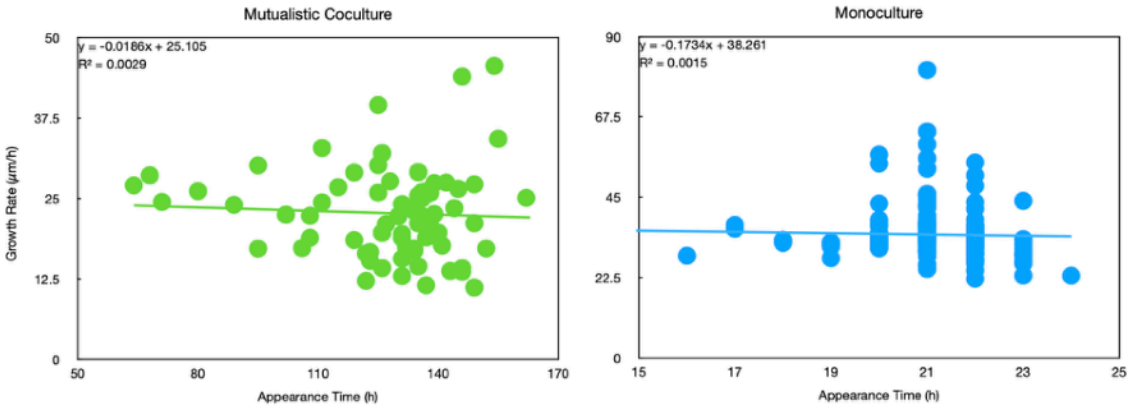

Figure S5. Little Correlation between Growth Rate and Appearance Time (i.e. Lag Time) of *E. coli* on Surfaces. Each line was a linear line of best fit between appearance time and lag time of each *E. coli* colony on the mutualistic coculture agar (Adjusted R^2=-0.012, p=0.6614) and on the monoculture agar (Adjusted R^2=-0.00348, p=0.5826).